5-29-2012

Design and Pilot Biomechanical Evaluation of a New Device for the Surgical Treatment of Atlanto-Axial Instability

Darren Lee Davis

DESIGN AND PILOT BIOMECHANICAL EVALUATION OF A NEW DEVICE FOR THE SURGICAL TREATMENT OF ATLANTO-AXIAL INSTABILITY

By

Darren Lee Davis

A Thesis

Submitted in Partial Fulfillment of the

Requirements for the Degree of

Master of Science

Major: Biomedical Engineering

The University of Memphis

August 2012

Acknowledgments

I extend my thanks to Dr. Peter Robertson for providing me with the opportunity to work with him as we have developed the BTS implant. Dr. Robertson has provided me an increased knowledge of the requirement for the stabilization of the C1-C2 motion segment. I also extend my thanks to Medtronic, and in particular to Roy Lim, Director of International Engineering, for providing me a key principal role in designing of the BTS device and testing. It has also been my pleasure to work with Dr. Eugene Eckstein as my advisor as I have completed my Master's program in Biomedical Engineering. Dr. Eugene C. Eckstein has provided me with a better understanding of how engineering principles can be applied to medical indications. Also, I extend my appreciation for the time spent by Dr. Denis J Diangelo and Dr. Gladius Lewis as my thesis committee members, who have been gracious to provide guidance with my topic.

ABSTRACT

Davis, Darren Lee. M.S. The University of Memphis. August 2012. Design and Pilot Biomechanical Evaluation of a New Device for the Surgical Treatment of Atlanto-Axial Instability. Major Professor: Eugene C. Eckstein, Ph.D.

The purpose of this paper was a biomechanical review of a new device, BTS (Bilateral Transarticular Spacer), to stabilize atlanto-axial motion. The biomechanical performances of the BTS and Harms technique were compared using 6 cadaver spines. The BTS was also designed to lessen the risks of damaging life sustaining nerves and arteries during placement at the atlanto-axial joint.

Two hypotheses were postulated: 1.) The BTS will be able to stabilize the atlanto-axial joint after a type-2 odontoid fracture; and 2.) BTS will function biomechanically similar to the traditional Harms stabilization technique.

In conclusion, the testing performed provided initial feasibility evidence that the new BTS device reduced atlanto-axial motion ($p < 0.01$) and provided stabilization similarly to the Harms technique ($p < 0.01$) with loads of 1.5 Nm in flexion-extension, axial rotation, and lateral bending.

TABLE OF CONTENTS

LIST OF TABLES

Table **Page**

LIST OF FIGURES

Figure **Page**

KEY TO SYMBOLS OR ABBREVIATIONS

AA …… Atlanto-Axial

AAI …… Atlanto-Axial Instability

AR …… Axial Rotation

FE …… Flexion-Extension

LB …… Lateral Bending

OC …… Occipitocervical

ROM …… Range of Motion

VA …… Vertebral Artery

VAF ……Vertebral Artery Foramen

INTRODUCTION

Clinical Problem

The anatomical stability of the human spine is complex and dependent on the interrelationship among muscles, tendons, joints, cartilage, bone, and ligaments. Damage to these structures can lead to instability of the spine. Clinical atlanto axial instability (AAI) arises when joint motion compromises neurological, muscular, vascular, and/or other physiological structures due to excessive range of motion (ROM).[1] The atlanto axial (AA) motion segment is comprised of two vertebral bodies known as C1 and C2. The dimensional relationship of the AA motion segment has been documented in the normal/non-symptomatic adult population. Two relationships that are significantly related to AAI are measured in the sagittal plane as illustrated in Figure 1. The first of these two dimensions is measured from the posterior portion of the anterior ring of C1 and the anterior portion of the odontoid. This dimension is normally between 3-4 mm, and the clinical situation is considered unstable when this dimension exceeds 4mm. The second of these is the measurement between the posterior portion of the odontoid and the anterior portion of the posterior C1 ring. This is the distance across the spinal canal and is considered abnormal when less than 13mm.[1]

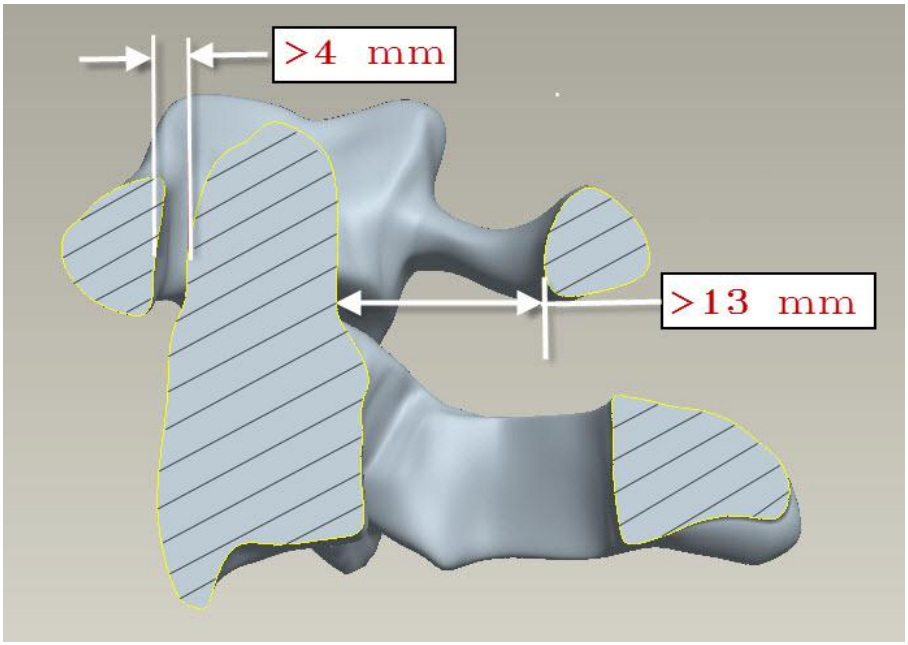

Figure 1. Normal adult C1-C2 dimensions, sagittal view.

Incidence of Clinical Problem and its Surgical Solution

The causes of AAI are manifold, e.g., traumatic fracture, ligamentous laxity, rheumatoid arthritis, and congenital disorders.[2] As a result of these circumstances, misalignment of the C1-C2 vertebras can occur, which lessens the ability of the spine to provide several important functions such as posture and protection of the spinal cord. When such functions are compromised, severe pain or even death can result. Spinal surgery to temporarily stabilize such spinal damage is also risky. Beyond risks like anesthesia, atlanto-axial surgeries are complex because the spinal cord, spinal nerves, and the vertebral arteries are interwoven with the spaces among the atlanto-axial joint, which makes implantation of stabilization devices difficult. Temporary fixation of the vertebral bodies to provide a means for fusion in a position that permits function of blood vessels and nerves is the current surgical process to solve this clinical problem.

Current Surgical Indications and Contra Indications

AAI is an indication for the reduction and fusion of the AA motion segment and is typically diagnosed by identification of subluxation radiographically. One current surgical technique in the stabilization of AAI is the Magerl technique.[3] Another surgical technique used in the treatment of AAI is the Harms technique. Both of these surgical techniques are considered "Gold Standard" treatments for C1-C2 AAI.[4,5] Both techniques have contra indications when the patient's vertebral artery placement and/or neurological anatomy are in immediate danger when placing fixation screws.[4]

Proposed Work and Comparison to "Gold Standard" Techniques

There are several mindsets in the evaluation of the performance of medical devices like these. Many of the tests used in providing evidence to the FDA in the submission of new medical devices are standards developed by ASTM. The applicable non-cadaveric ASTM test for a posterior fixation device such as for the Harms technique would be ASTM F-1717, which measures aspects related to compression and torsion. For an inter-body device, the associated testing would be F-2077 for compression, torsion, and shear loadings. This new device, BTS, is a hybrid, possessing a posterior plate and a wedge feature used as an inter-body spacer. These tests could provide evidence under controlled circumstances that a device performs equivalently to or better than currently available devices. These ASTM tests specifically communicate that they are not intended to determine in-vivo efficacy. Since the BTS and Harms devices do not share a similar ASTM test method, it was decided to conduct a cadaveric spine study.

There are many variations of human anatomy such as bone quality, size, and shape that cannot currently be fully evaluated by ASTM tests. Human cadaver testing

can provide a fuller understanding of the interactions of these medical devices with examples of human anatomy but still cannot replicate clinical use. Care must be taken in the selection of cadaver spines for this type of testing so as to not use degenerative spines. Use of a spine which incurred trauma or had fusion between motion segments would create unusable information for this type of study. Use of spines with degenerative conditions would create another variable that could create variations of individual spine performance and thereby skew or misrepresent test results. Equipment used to apply loads to cadaver spines to evaluate the performance of implants varies between labs as well. The test results shown here were acquired at Dr. Avinash G. Patwardhan's Musculoskeletal Biomechanics Laboratory, Edward Hines, Jr. VA Hospital. The testing method for this lab was designed to closely approximate a pure bending moment with a minimal axial force applied to the cervical spine.[6] A pure bending moment test is ideal to compare the biomechanical properties of rotational stiffness between different spine conditions.

This biomechanical evaluation of the BTS to temporarily stabilize the AA motion segment is of combined interest for the collaboration between Medtronic and Dr. Peter Robertson. To simulate AAI, a type-2 odontoid fracture was used to destabilize this motion segment. The use of an odontoid fracture is consistent with published scientific journal articles studying the effects of instrumentation on AAI.[5,7-12] The six cadaver spines tested in this study provide measurements of flexion-extension (FE), lateral bending (LB), and axial rotation (AR). Prior to instrumentation of the Harms and BTS technique, the intact spine was tested to provide a baseline. After the spines were tested with the Harms and BTS technique, both with a broken odontoid to simulate the

destabilized condition, the spines were tested in the destabilized condition without any these devices.

Purpose and Goals of the Study

The purpose of this study was to compare the biomechanical performance of the BTS and Harms devices to stabilize atlanto-axial instability. The need for such a device was derived from the surgical complications associated with the variation in anatomical location of the vertebral artery foreman (VAF) and lack of available bone mass purchase for anchoring screws. These two factors create surgical risks when utilizing current "Gold Standard" procedures.[5] Criteria for evaluating the BTS device included a) reducing the risk of impacting the vertebral artery (VA) and b) providing stabilization between C1-C2 similar to the Harms technique. To reducing the risk of screws or drills penetrating the VAF, it was determined to address two factors: increase visualization of the implant placement during surgery and provide a placement geometry for the implant that is as medial to the spinal canal as possible. An unrelated device used by Atul Geol, M.CH in the implantation of spacers alone in the AA joint revealed that a posterior technique is relatively straightforward and avoids the VA.[13] Over a period of time through discussions with Dr. Peter Robertson, implant specifications were determined. Once a functional BTS design was created it was tested at Dr. Patwardhan's lab in Chicago to evaluate how it performed in FE, AR, and LB as compared to the Harms technique.

Functional Anatomy Physiology of Human Upper Cervical Spine

The BTS device is intended to be surgically located in the Atlas (C1) and Axial (C2) motion segment to limit its motion. The relationship between connecting spine anatomy is discussed below because the atlanto-axial motion segment is affected by adjoining vertebrae and connective tissue.

The spine is subdivided into four major groups: cervical, thoracic, lumbar, and sacrococcygeal. These segments are illustrated in Figure 2 and are distinguishably different by observing the change in curvature between these four spine regions.

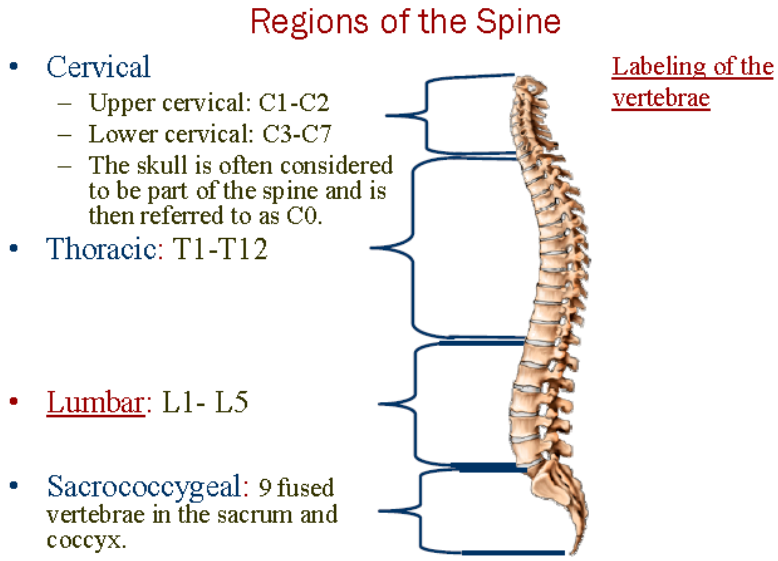

Figure 2. Regions of the Spine.
Source: Schnuerer, A.P., & Gallego, J.M. (1998). Basic Anatomy & Pathology of the Spine. Memphis: Medtronic.

The vertebral bodies and connective tissue within each of these four groups of vertebra have similar features. Vertebras are named with an alpha-prefix identifying their region of the spine and are numbered sequentially cranially towards caudal. The C1-C2

motion segment is part of the upper cervical vertebrae as illustrated in Figure 3. A motion segment consists of two adjacent vertebrae and connecting ligamentous tissue which provides for the motion of the spine.[1]

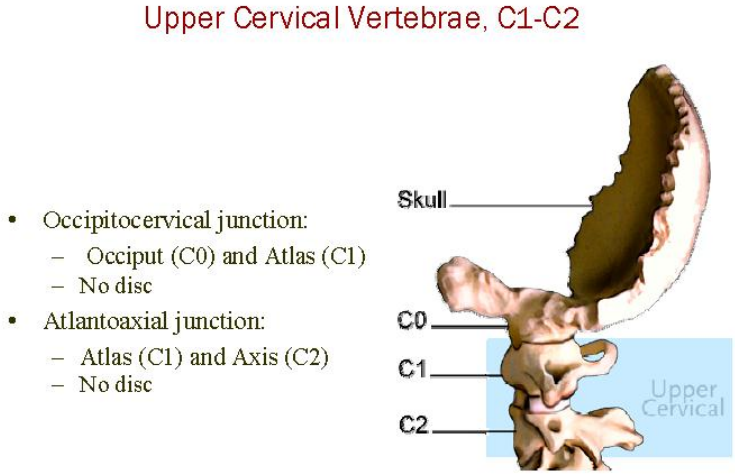

Figure 3. Upper Cervical Anatomy.
Source: Schnuerer, A.P., & Gallego, J.M. (1998). Basic Anatomy & Pathology of the Spine. Memphis: Medtronic.

The occipitocervical (OC) junction is a group of motion segments located most cephalad in the cervical spine which consists of the base of the Skull (C0), atlas (C1), and Axial (C2) vertebrae. The cervical spine is comprised of 7 vertebrae connected to one another via 14 facet joints, 5 discovertebral joints, 10 neurocentral joints, 33 synovial articulations, 2 occipito-atlantal joints, one atlanto-dental joint surrounded posteriorly by contact with the transverse ligament. The contact points between vertebras are known as joints. The C0-C1 motion segment, has two symmetric bilateral joints known as the occipitocervical joint. As can be seen from Figure 4, this joint has a ball and trough feature that is ideal as a pivoting joint.

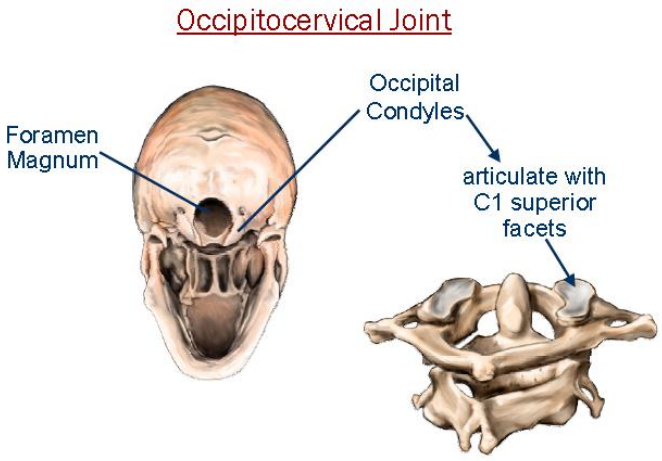

Figure 4. Occipitocervical Joint.
Source: Schnuerer, A.P., & Gallego, J.M. (1998). Basic Anatomy & Pathology of the Spine. Memphis: Medtronic.

The C1 and C2 bony anatomy is further illustrated in Figure 5 and Figure 6. The odontoid of C2 passes cranially through the Atlas, C1.

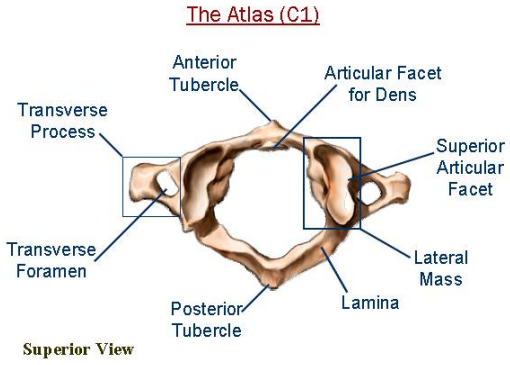

Figure 5. C1 Bony Anatomy.
Source: Schnuerer, A.P., & Gallego, J.M. (1998). Basic Anatomy & Pathology of the Spine. Memphis: Medtronic.

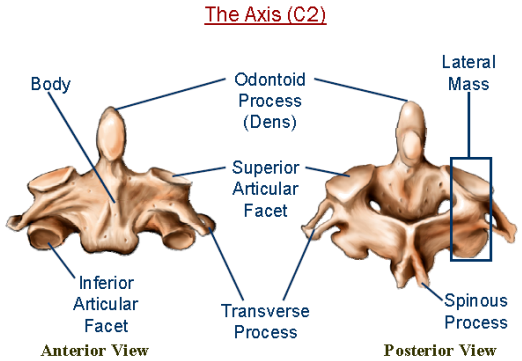

Figure 6. C1-C2 Bony Anatomy.
Source: Schnuerer, A.P., & Gallego, J.M. (1998). Basic Anatomy & Pathology of the Spine. Memphis: Medtronic.

These two vertebral bodies are arranged as shown in Figure 7 and are known as the AA motion segment. The C2 superior articular facets as shown in Figure 6 contact the

inferior surface of C1 to form facet joints. These facet joints are each encapsulated with an annulus containing synovial fluid and known as the facet capsules. For the purpose of the associated testing to evaluate the fixation properties of the BTS design, a type-2 odontoid fracture was created on cadaveric spines before measuring motion of the instrumented AA motion segment. The odontoid process, also known as the Dens, is shown in Figure 7. Odontoid fractures can be identified by 3 types of breaks as illustrated in Figure 8. The BTS spacer body will transect the AA articular joints also known as the zygapophyseal joints.

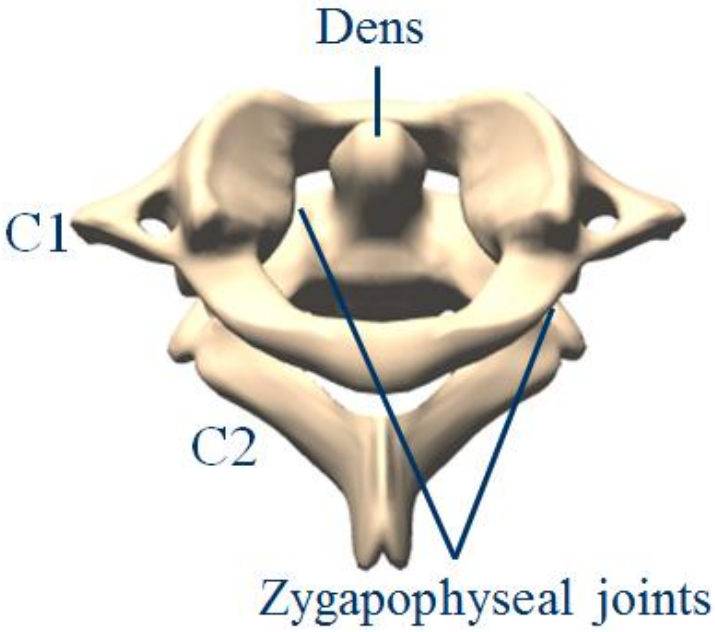

Figure 7. C1-C2 Assembly
Source: Schnuerer, A.P., & Gallego, J.M. (1998). Basic Anatomy & Pathology of the Spine. Memphis: Medtronic.

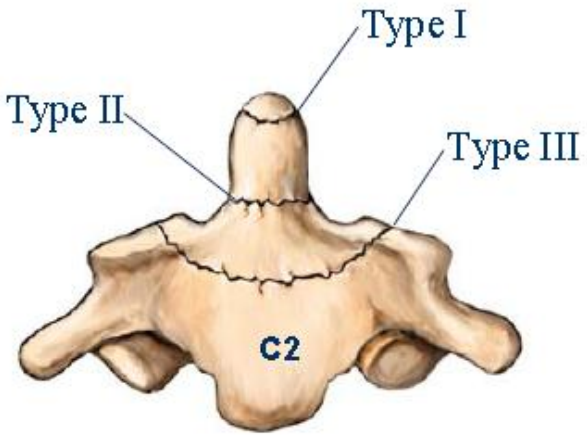

Figure 8. Odontoid Type Fractures.
Source: Schnuerer, A.P., & Gallego, J.M. (1998). Basic Anatomy & Pathology of the Spine. Memphis: Medtronic.

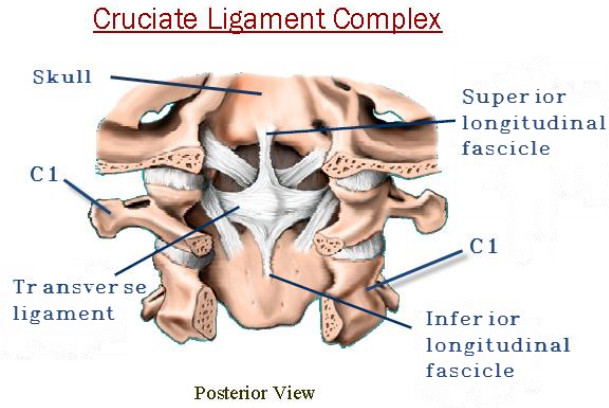

Figure 9. Cruciate ligament.
Source: Schnuerer, A.P., & Gallego, J.M. (1998). Basic Anatomy & Pathology of the Spine. Memphis: Medtronic.

The intact odontoid process provides stability to the AA motion segments in several ways. The atlanto-dental joint articulates with the posterior portion of the anterior C1 ring and is captured posteriorly by ligaments known as the cruciate ligament complex. This complex ligament structure can be seen in Figure 9. The odontoid is captured by surrounding ligaments and provides a fixation point for the Apical and Alar ligaments which connect C2 with C0 as pictured in Figure 10. A type-2 odontoid fracture will simulate AAI and also destabilize ligamentous structures that are associated with C0-C1 motion.

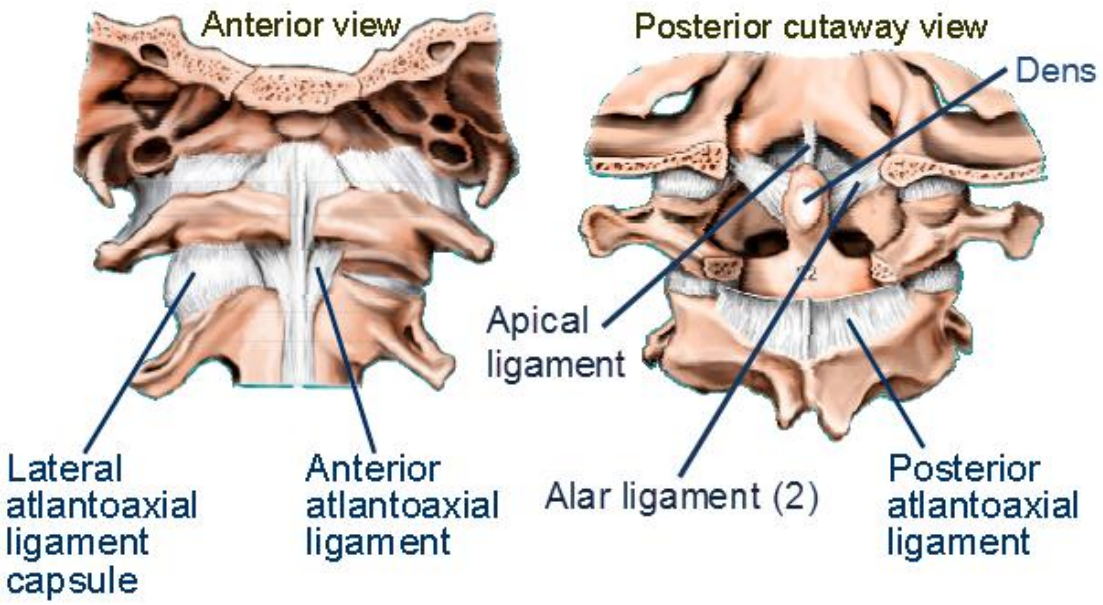

Figure 10. C0-C1-C2 Ligamentous structures. Source: Schnuerer, A.P., & Gallego, J.M. (1998). Basic Anatomy & Pathology of the Spine. Memphis: Medtronic.

Other ligaments pass through and attach to C0, C1, and C2 vertebra such as the anterior and posterior longitudinal ligaments. These structures provide for a more continuous support throughout the entire spine. The nuchal ligament also passes alongside the C1-C2 motion segment. It is located posterior to the C1-C2 motion segment. It is affixed to the occipital bone of C0 and the posterior tubercle of C1 as it passes inferiorly to the adjoining C2-C7 vertebral spineous processes. The importance of the ligaments as related to the odontoid process will be demonstrated from the testing utilizing the type-2 odontoid fracture. It will be shown that when only a limited number of these ligaments are compromised, instability will increase substantially. Ligaments are flexible to bending but exhibit rigidity to stretch, which are ideal properties needed to limit joint motion. Their attachment to the outside covering of bony anatomy know as cortical

bone, provides good anchor points to limit hyper-flexed or hyperextended joints. When these structures are compromised, loads applied to the spinal column can produce subluxation, over rotation, or extreme motion of vertebral bodies and the resulting misalignment can cause severe neurological injury or death.[1,2]

Kinematics and Measurements of the Cervical Spine

The OC Joint is one of the most complex motion segments of the spine. This two level complex joint provides for the majority of the flexion-extension (yes-motion response) as well as axial rotation (no-motion response). The C0-C1 motion segment provides more than 50% of the flexion-extension of the cervical spine because of the anatomical shape of the interface between C0 and C1. The possible motion of the spine is first controlled by the shape of the contact points between the vertebral bodies. The AA motion segment provides more than 50 % of the axial rotation of the cervical spine.[2]

Several research groups have published comparisons between implants used in the stability of AAI. There are several consistent themes among these publications. (1) Measuring the ROM of FE, LB, and AR in cadaveric spines, (2) an applied test loads of ±1.5 Nm, (3) and the use of an odontoid fracture to simulate AAI.[5,7-12] As a result, the BTS testing utilized all three of the aforementioned criteria.

The in-vivo AA ROM has been measured in previous studies and is provided in Table 1. Although differences between the measured motions exist, the studies indicate that the primary motion attributed to this joint is axial rotation.

Table 1. Ranges of FE, LB, and AR Reported in Degrees (Mean ± Standard Deviation) for the C1-C2 Motion Segment

	Flexion+Extension	Lateral Bending (one side)	Axial Rotation (one side)
Dvorak [14] *In vivo*	15.0±3.0		43.1±5.5
Panjabi [15] *In vitro*	22.4±4.7	6.7±4.4	38.9±5.4
White and Panjabi [1]	20.0	5.0	40.0
BTS testing (Results from this Patwardahan testing, 2010)	14.1±2.9	1.8±1.1	33.65±6.9

Techniques of C1-C2 Fixation

Over the past century techniques for stabilizing AAI have evolved from early simple wiring techniques. Today, the standard of care requires surgical techniques that support the biological response to fuse the damaged joints. The following techniques provide a brief history from wiring to screw fixation techniques of the atlanto-axial joint.

Gallie

The Gallie technique was developed in 1939 as a posterior wiring technique. This technique involves the placement of a surgical wire looped around the posterior spineous processes with the intervention of a bone graft to maintain distraction and lordotic angle between the AA motion segment. The wire restricts flexion and the bone graft restricts extension in the sagittal plane.[16] The problem with this technique is it provides only a

focal fixation connection between C1 and C2. This type of construct is very effective in restricting motion in the sagittal plane but less effective in restricting lateral bending or axial rotation motion.[7] Although this surgical technique is limited in restricting motion of AAI, it is not as dangerous to implement as techniques that require placement of lateral mass or transarticular screws since it is a posterior approach and is distal to the spinal cord, exiting C1 nerve roots, and VA.

Magerl (Trans-articular screw fixation)

The Magerl surgical technique was developed in 1979 by Magerl and Seeman[7] which utilized the Gallie wire technique in combination with two transarticular screws to provide for improved fixation. Due to the location of the two transarticular screws, and the binding by the wire and the bone insert, this technique can restrict all six AA motions: FE, LB, and AR. It is currently one of the "Gold Standard" surgical techniques used for stabilizing C1-C2 motion.[7] This technique is one of Dr. Robertson's choices as well as other neurosurgeons when addressing patient care. This surgery presents risks due to the close proximal placement of transarticular screw with the VA as well as the sub-laminar Gallie wire placement. As can be seen from a surgery conducted by Dr. Robertson in Figure 11, the starting drill point to maintain the trajectory through the AA joint is dramatically caudal to the AA motion segment. This situation causes limited visibility of the drill point which can lead to unintentionally damage to the VA, or C2 exiting nerve root, or the spinal cord, any of which can be catastrophic. Another variable is the variation in location of the VAF at the AA segment. This image also demonstrates how curvatures in the lower cervical and thoracic regions can constrain surgical methods. It is necessary to do surgical planning to determine the location of a patient's VA prior to

surgery to determine if bone screw technique such as the Magerl or Harms are possible. It has been found that this technique has high rates of exclusion as a surgical solution of AAI due to VAF location.[10,17,18]

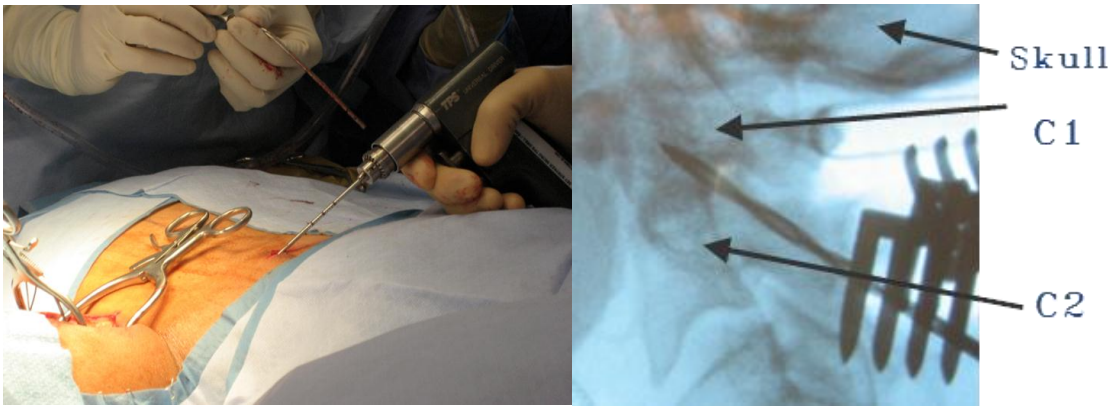

Figure 11. Magerl Surgical Technique. (Left) Surgical drilling of C1-C2 vertebra for transarticular screw placement. (Right) CT scan with drill transecting C1-C2 articulating joint.

Harms (C1 lateral mass screw and C2 pedical screw fixation)

Another "Gold Standard" surgical technique used for stabilizing AA motion is the Harms technique, which utilizes two C1 lateral mass screws and two C2 pedicle screws attached with two bilateral spinal rods as illustrated in Figure 12.

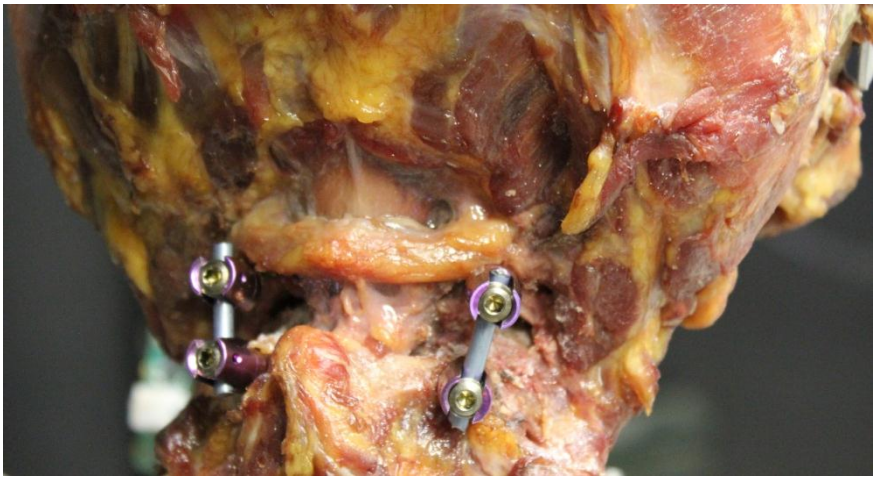

Figure 12. Harms Surgical Technique. Posterior view of the Occipital-Cervical Junction with soft tissue removed.

This technique was published in 2001 by Harms and Melcher with the results of 37 patients who underwent this surgery. It was reported that fusion rates are nearly 100% with this technique.[18] It has been estimated that the Harms technique can contribute to VA injury at 4.1% per patient or 2.2% per screw placement. Also, neurological injuries were reported at 0.2% per patient or 0.1% per screw. These injuries result in a mortality rate of 0.1%.[7]

Shortcomings of Current Techniques

All surgeries pose some level of patient health risks but AA stabilization surgery has specific risks including VA and neurological damage. These surgeries require the avoidance of the (1) spinal cord, (2) C1-C2 exiting nerve roots, and (3) vertebral artery. The danger for screw placement arises when the VA is located too medial which decreases the safe zone between the bone screws and VA. It has been reported that abnormality of the VAF location has been observed in 23% of the population.[10] Limited

bone mass also presents an issue when trying to locate the fixation screws. Dr. Peter Robertson studied the limitations of the currently available AAI stabilization techniques. He has found in an evaluation of 30 patients that 7 out of 60 Magerl screws and 5 out of 60 Harms screws could not pass without transgression of the VAF.[17] The BTS design has the ability to mitigate some of the VAF issues associated with stabilizing AAI. These concerns provide the impetus for developing the BTS.

BTS Design Considerations

By design, the BTS implant is intended for a direct posterior surgical approach. Several features of the implant are illustrated in Figure 13 and are discussed below. The BTS includes two main body features: the main body that serves as an articulation joint spacer which is surgically placed within the facet capsule and the posterior flange that allows fixation with the C2 lamina. The joint spacer provides for a C1 fixation screw trajectory and an area to place bone graft materials. The posterior flange provides for two small bone screws to attach with the C2 lamina. The new device construct is comprised of bi-lateral C1-C2 BTS implants (left and right mirror implants), two bone screws placed bi-cortically through the C1 lateral mass, and four small C2 lamina bone screws. The BTS implant is designed for placement in as medial a location as possible without narrowing the VAF. So the design of the main body is narrow to avoid contact with the VA, and yet sufficiently wide to provide for an angled flange to mate anatomically with the C2 lamina. The C1 and C2 screw trajectories are chosen to avoid transecting areas associated with the VAF. Another design consideration related to the implanted position is to limit possible abrasions of the nearby C1 exiting nerve roots. The implant possesses

a bull nose tip to improve insertion and serrated contact surfaces for the articulating joint interface to reduce implant migration once it is implanted.

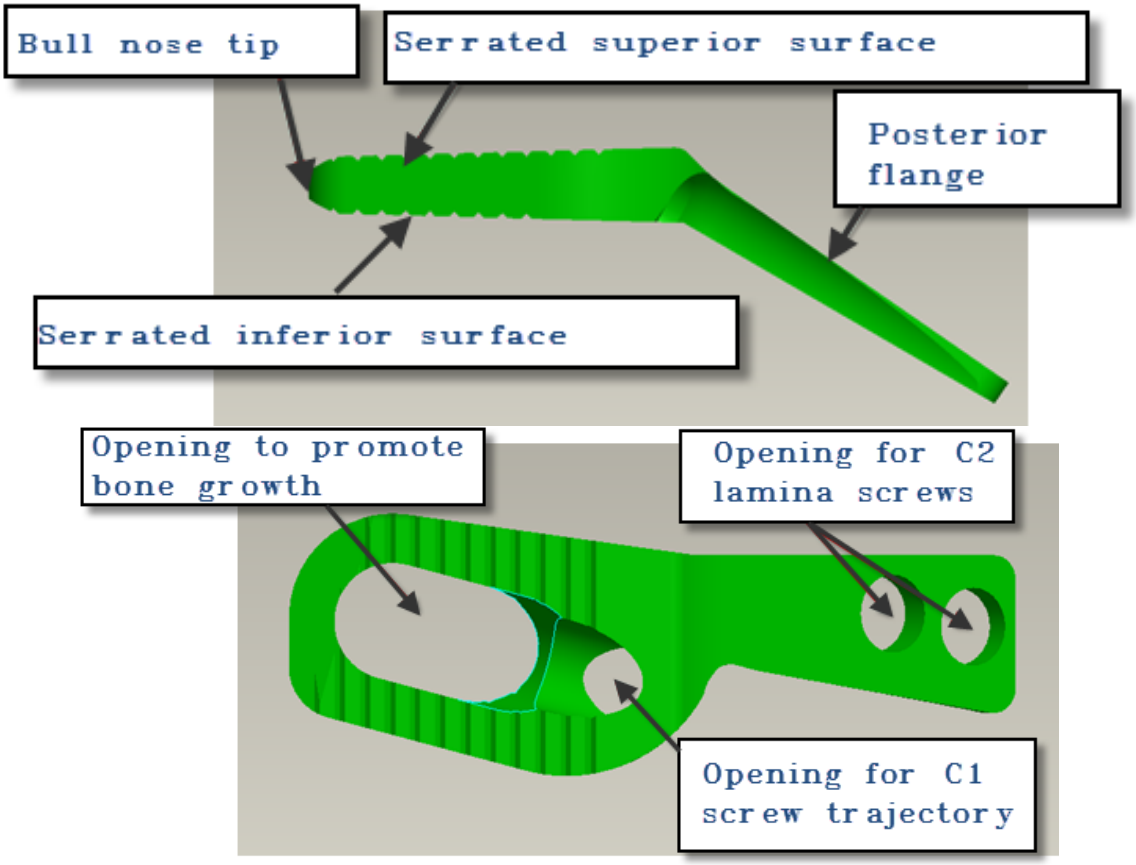

Figure 13. (top) BTS side view and (bottom) BTS top view illustrating features. The label "Opening to promote bone growth" represents an area that will permit a surgeon to place bone graft or other materials to promote bone growth.

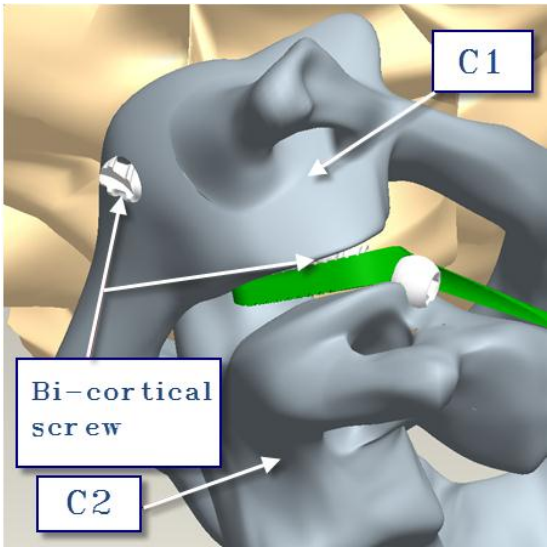

Figure 14. Illustration of BTS implant side view with bones showing C1 bi-cortical screw trajectory.

Choices of C1 bone screw lengths are the responsibility of the surgeon, decides in the clinical setting so as to ensure bi-cortical fixation to the C1 vertebra for each patient's anatomy. (See Figure 14) An unnecessarily long screw may affect nearby anatomy such as the throat. The trajectory of the C1 bone screws are critical to ensure the device can provide stabilization of the AA motion segment. Too shallow of a trajectory with respect to the AA joint can lead to the bone screw breaching the inferior surface of the C1 vertebra during placement of the screw.

The BTS surgical technique involves a posterior approach to the AA motion segment with a midline incision and tissue retraction. Visualization of the bifid C2 spineous process will provide for a landmark for locating the C2 pars interarticularis as well as the articulation joint. Partial resection of both facet capsules with a curette will prepare a space for the location of the main body of the BTS spacer. Tissue is then removed from the C2 lamina for interface with the BTS flange. The BTS implant is impacted into the AA articulation joint and secured with both C1 and C2 screws. The final instrumented spinal construct is pictured in Figure 15 prior to C1 and C2 bone screw attachment.

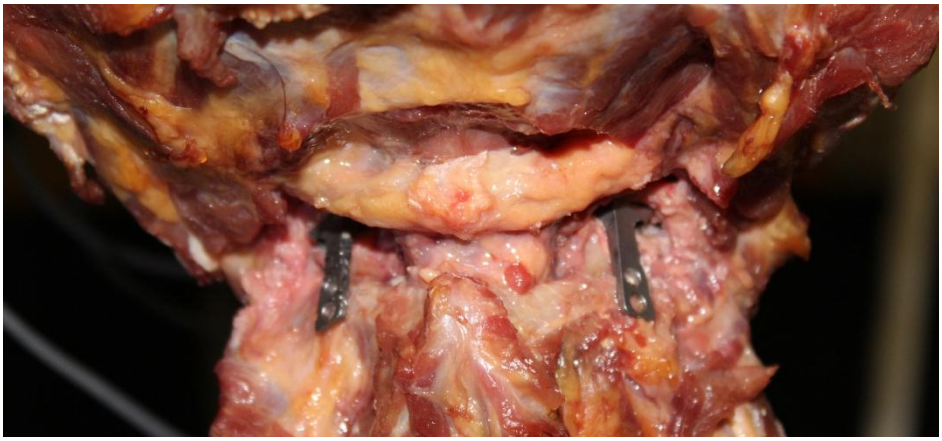

Figure 15. Illustration of the BTS implant. Posterior view of the Occipital-Cervical Junction with soft tissue removed.

Each spacer will transect the AA articular joint with the posterior flange laying on the superior C2 lamina. The BTS implants will be located as medial as possible without narrowing the spinal canal foreman as reflected in Figure 16 (right).

Figure 16. (left) Illustration of some decortication of the superior surface of C2 vertebra due to implant insertion. (right) Illustration of the BTS implant still affixed to inferior surface of C1 vertebrae.

Future design considerations include minimizing abrasions with the nerve roots that exit near the AA joint. The C1 exiting nerve root lay slightly superior to the junction between the articulating joint spacer and the posterior flange. This location is also occupied by the head of the C1 bi-cortical screw. It is important to ensure this contact area is smooth and without sharp edges. The implant should provide a means to restrict both the C1 and C2 bone screws from backing out. Also, the implant needs to be designed in such a way to allow intimate mating with an inserter and drill guide instrument.

Height

The main body of the implant which separates the AA articulating joint must be provided in several heights. Inadequate height to mimic spacing present in the original anatomy will simulate a collapsed joint and not maintain proper ligament tension, which could permit subluxation and impingement of nerve roots, vertebral artery, and possibly the spinal cord. Overly large implant height will create over distraction of the AA joint causing tension of surrounding anatomy. This over distraction can result in nerve damage.

Material of Construction

The implant and screws are made from Titanium alloy, Ti-6Al-4V, ASTM F136, which is a workhorse material, widely used in the manufacturing of spinal implants and has proven biomechanical stable for cervical spinal indications.

Advantages of BTS vs. Harms

The fluoroscopy images in Figure 17, illustrate the difference in location as viewed in the sagittal plane between the BTS and Harms. The BTS has several benefits when

compared to the Harms. The BTS provides for inter-body support that provides stability by distraction of the joint. Upon insertion the BTS immediately provides noticeable spinal stabilization even before any screws are attached. This stabilization occurs as a result of annular tension from ligaments connecting C1 and C2 together. This annular tension stabilization is also reflected in the use of C1-C2 spacers which do not utilize fixation screws.[13] Another obvious improvement is the reduced profile and lessened amount of metal.

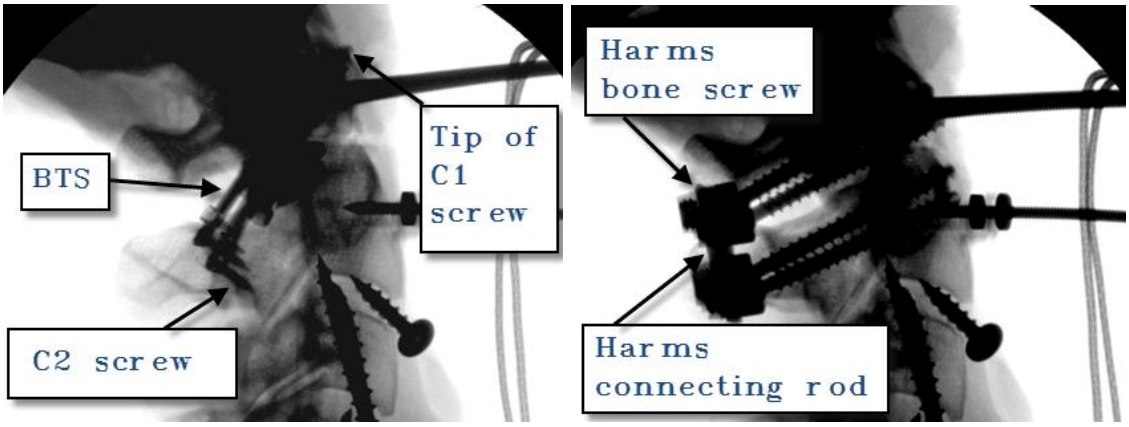

Figure 17. Fluoroscopy images of (left) BTS and (right) Harms instrumentation.

Loading comparison between the BTS vs. Harms

The following analysis provides loading scenarios for the BTS and Harms devices in FE and AR. This analysis neglects any load sharing between these devices with associated anatomy as well as axial loads applied by this test method. A LB analysis was not considered in this review due to the limited motion of the AA joint in lateral bending.

FE analysis for the BTS

The BTS device could experience numerous types of loading conditions at the superior surface of the implant. Two different FE loading conditions between the inferior surface of the C1 vertebral body and the superior BTS surface/C1 bone screw interface are analyzed. The first (1) condition can occur when the C1 screw does not reduce the C1 vertebra completely, which creates a gap between the inferior surface of the C1 vertebra and the superior surface of the BTS blade. Assuming no C1 axial preload and the C1 screw can toggle freely within the BTS body. Assume no inferior C1 vertebra subsidence on the BTS implant which would cause a load at the tip of the implant (assumed a point load) as illustrated in Figure 18. Since the BTS implant is installed bilaterally, the 1.5 Nm applied load is divided by two.

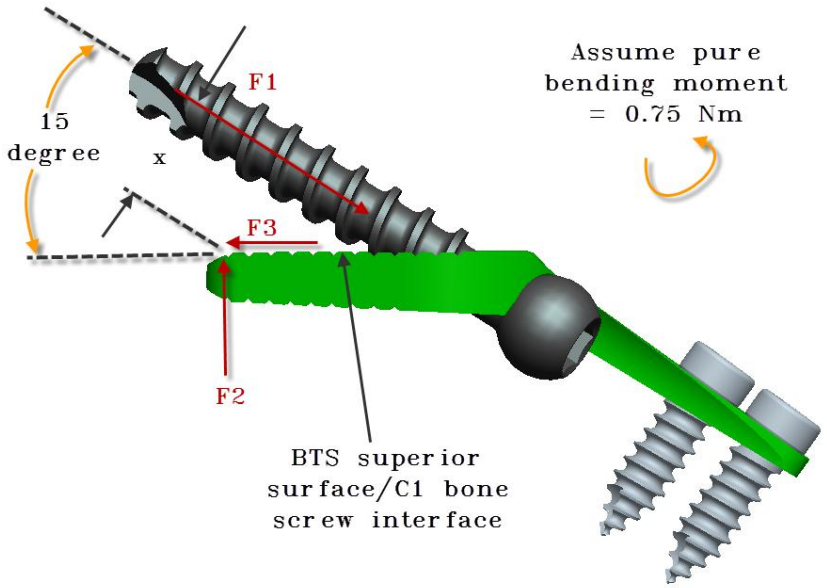

Figure 18. FBD, BTS condition 1 (flexion)

The resultant forces are calculated from equations 1 through 3. The C1 screw would be in pure tension as a result and the tip of the implant in compression.

$$\sum M = 0$$

$$F1 * X = 0.75\ Nm \qquad (Eq. 1)$$

$$\sum F = 0$$

$$F2 = F1 * Sin15°\ Nm \qquad (Eq. 2)$$

$$F3 = F1 * Cos15°\ Nm \qquad (Eq. 3)$$

The second condition (2) can occur when the C1 screw does not completely reduce the C1 vertebra, which creates a gap between the inferior surface of the C1 vertebra and the superior surface of the BTS blade. The C1 screw has rotated to the endpoint within the BTS implant due to AA joint extension. Assume that the BTS implant is strong enough to support the C1 screw and the failure mode is the minor diameter of the C1 screw. The C1 screw is carrying all the bending moment as illustrated in Figure 19.

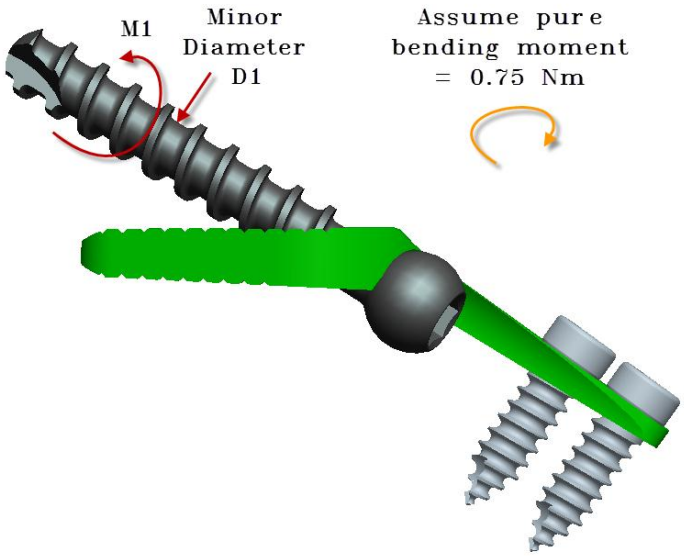

Figure 19. FBD, BTS condition 2 (extension)

The resultant stress on the minor diameter for condition 2 can be calculated from equations 4 through 6. This will produce a worst case condition in comparison with condition 1 because the minor diameter is resisting all the bending moment. Condition 1 would only be resisting a tensile force on the minor diameter and utilizing the BTS blade to create an offsetting force.

$$\sum M = 0$$

$$M1 = 0.75\,Nm \qquad (Eq.4)$$

$$I\ (Moment\ of\ Inertia) = \frac{\pi(\frac{D1}{2})^4}{4} \qquad (Eq.5)$$

$$\sigma = \frac{M1 * (\frac{D1}{2})^4}{I} \qquad (Eq.6)$$

The BTS device also transfers the FE loads between the (qty=2) C2 screws and flange to the lamina of the C2 vertebra. The worst case loading is an extension load for this interface as illustrated in Figure 20. For simplicity sake Fc is illustrated as a point force. In reality, the C2 lamina surface is not planar and will create a gap at the tip or other various locations between the BTS flange and the C2 lamina. As a result, the a and b dimensions will decrease as Fc locates at a solid C2 surface interface as well as distributing the Fc force about an area between the flange and C2 lamina.

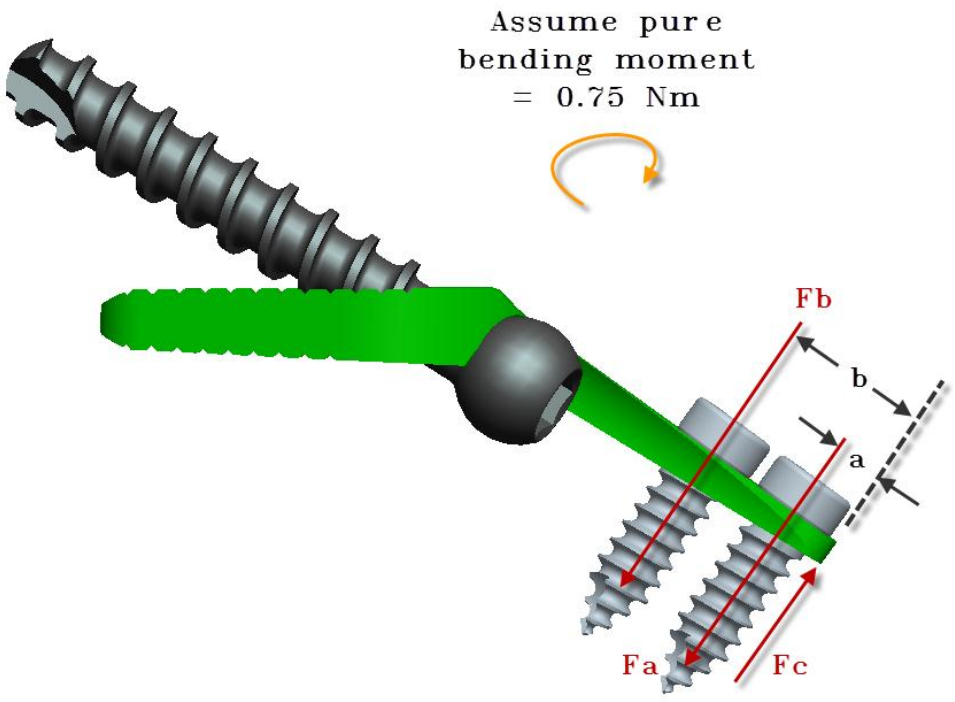

Figure 20. FBD, BTS C2 screw/flange interface (extension)

The resultant C2 bone/screw pull-out forces can be calculated from equations 7 and 8. The BTS design will benefit in this loading condition by increasing both dimensions (a) and (b) as much as possible while still providing good bone purchase/interface with the C2 lamina.

$$\sum M = 0$$

$$(F_b * b) + (F_a * a) = 0.75\ Nm \qquad (Eq. 7)$$

$$\sum F = 0$$

$$F_a + F_b + F_c = 0 \qquad (Eq. 8)$$

Axial Rotation analysis for the BTS

The BTS implant will also need to stabilize axial loading because the AA joint is designed uniquely to provide axial rotation motion. Assuming the C1 screw has articulated to the endpoint within the BTS implant due to axial rotation forces of 1.5 Nm producing a resultant forces (Fd) on symmetrically placed BTS implants screws as illustrated in the Axial view of Figure 21. These loads will produce a shear force on the cross sectional area of the C1 screw. Since the screws are skewed to the load, the cross sectional area will increase due to the 15 degree angle it is placed with respect to the BTS implant as illustrated in the Left Side View of Figure 21. If the implants are both set apart a distance of (d), the shear forces as a result of the axial rotation of the neck can be calculated from equation 9. The shear force is translated through the BTS implant and is secured to the C2 lamina by the two C2 screws which also are in shear (Fe) as calculated

from equation 10. The shear force (Fe) is applied across the cross section of the C2 screws at their respective angle to the axial plane.

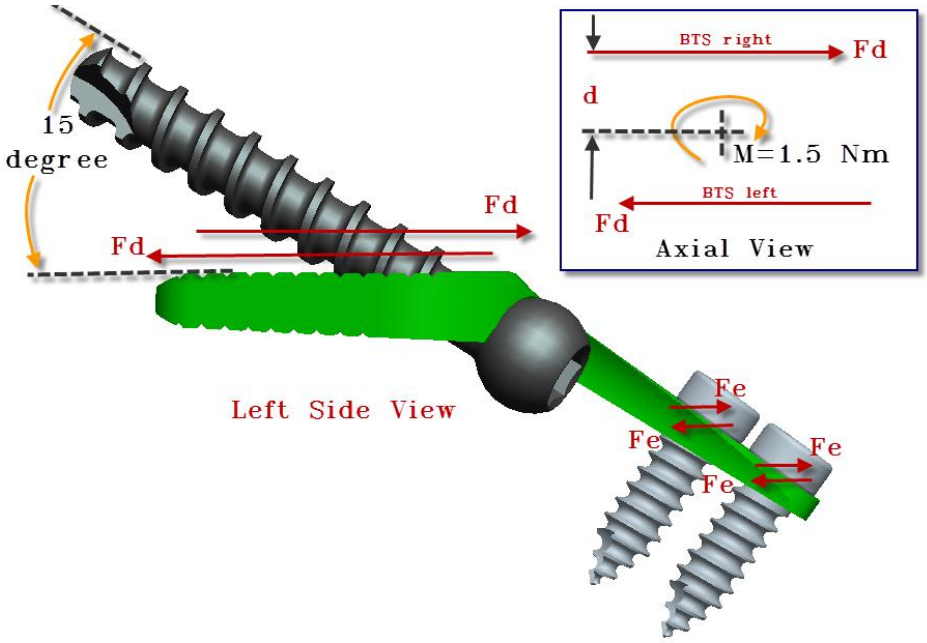

Figure 21. FBD, BTS C1&C2 screw/bone interface (axial rotation)

$$\sum M = 0$$

$$2 * (F_d * d) = 1.5\ Nm \qquad (Eq. 9)$$

$$F_e = \frac{F_d}{2} \qquad (Eq. 10)$$

Flexion Extension analysis for the Harms

This analysis also neglects any load sharing between the Harms device with associated anatomy and does not account for axial loading from the test method. The worst case stress for the Harms device is illustrated in Figure 22 at the minor diameter (D1) which possesses the smallest moment of inertia. The minor diameter for the Harms bone screw and the C1 bone screw used in the BTS device are the same diameter. As a result, when applied with only a pure bending moment of 0.75 Nm, the stress should be equivalent between screws with the same minor diameters. The benefit of the BTS construct vs. the Harms construct is the decreased length of the screw/rod carrying the bending moment. The BTS screw transitions from the BTS directly into the C1 bone with essentially no unsupported length while the Harms construct bone screw has an unsupported length of (y). As a result, the BTS will see less deflection due to the screw bending. The Harms construct also possesses a rod length (z) which will additional contribute to deflection as illustrated in Figure 22.

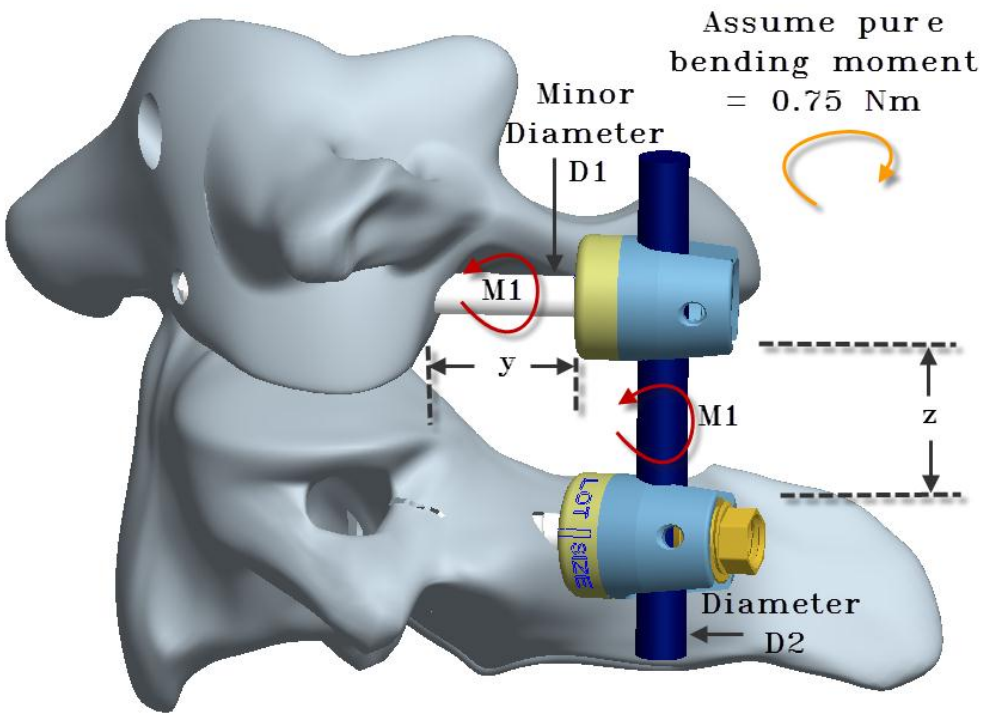

Figure 22. FBD, Harms (extension)

The primary motion associated with the AA joint is axial rotation. When the AA joint rotates, the anatomical geometry of the joint, which slops down anteriorly and laterally, causes the C1 vertebra to move cranially and caudally simultaneously as a result. If the motion of the neck is twisted, so as to face the eyes over the left shoulder, the left side of the C1 vertebra will translate cranially while the right side of C1 vertebra will translate caudally. The BTS spacer feature is beneficial in limiting this motion due to a wedging effect between the C1-C2 vertebras. Another benefit arises because portions of the BTS screws are set within the BTS body in shear as they are skewed in direction from the axial plane in which axial rotation occurs. The Harms bone screws have additional interconnection with components such as the 17.5 mm long 3.5 diameter rods which will produce deflection that is not found in the BTS. Each rod is not only in shear but also

experiences a bending moment as illustrated in Figure 23. The bending moment applied to the 3.5 mm rod is a result of the Force (F) multiplied by the 17.5 mm of separation between the bone screws.

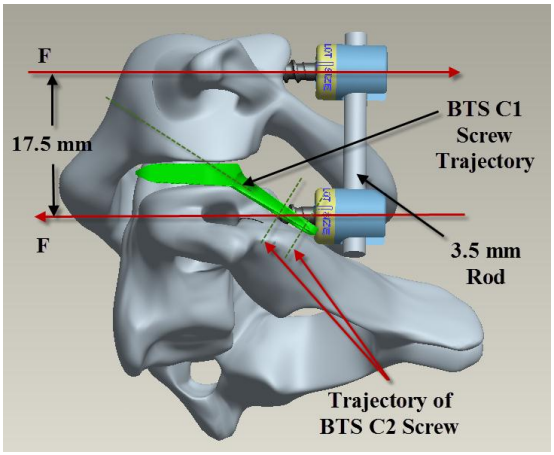

Figure 23. Dimensional comparison between the BTS and Harms in axial rotation.

Materials and Methods of Cadaveric Testing

The lab chosen to perform this evaluation of the BTS was at Dr. Patwardhan's Musculoskeletal Biomechanics Laboratory, Edward Hines, Jr. VA Hospital. This lab was chosen in light of their previous publications for cervical motion and prior work with Medtronic. The following materials were used in the BTS testing.

Materials

1) Six (6) Cadaveric spine segments (C0-C5) with the demographics listed in Table 2.

Table 2. Cadaver Spine Demographic Information

Specimen	Specimen #	Age	Sex	Cause of Death
3	C08001	59	M	Lung cancer
4	S090095	53	M	COPD
5	C070136	55	M	Cardiac arrest
6	C080913	49	M	Pancreatic cancer
7	GL100004	47	M	MI
8	S040646	65	M	Heart Failure

2) Steel plate

3) 120 cm rod for flexion extension test

4) 92 cm rod for lateral bending test

5) Acrylic cylinder, string, and pulleys for axial rotation test

6) Six-component load cell (Model MC3A-6-1000, AMTI Multi-component transducers, AMTI Inc., Newton, MA)

7) Optoelectronic motion measurement system (Model 3020, Optotrak®, Northern Digital, Waterloo, Ontario)

8) Three (3) bi-axial angle sensor (Model 902-45, Applied Geomechanics, Santa Cruz, CA)

9) Fluoroscopic imaging (GE OEC 9800 Plus digital fluoroscopy machine)

10) Two (2) positive displacement pumps

11) Six (6) Harms constructs built with the components listed in Table 3.

Table 3. Components Used in Harms Construct

Component Description	Qty/Construct
3.2 mm Ti Alloy Rod, 40 mm	2
Set Screw	4
3.5 X 32 mm Multi-Axial Screw	4

12) Six (6) BTS constructs built with the components listed in Table 4:

Table 4. Components Used in BTS Construct

Component Description	Qty/Construct
Left 3mm, BTS	1
Right 3mm, BTS	1
3.5 X 32 mm C1 screws	2
2.5 X 10 mm C2 screws	4

Methods

The setup activities performed for the following test methods were directed by Dr. Avinash G. Patwardhan. The surgical techniques were conducted by or overseen by Dr. Peter Robertson.

1) The Six (6) Cadaveric spines segments (C0-C5) were selected and prepared for this study. Radiographic screening was conducted to ensure cadaver specimens with spinal abnormalities were removed from this test. The criteria for exclusion included: specimens with fractures, metastatic disease, bridging osteophytes, or other conditions that could significantly affect the biomechanics of the spine. These specimens were thawed and soft tissue such as paraspinal

musculature was removed from the spine segment while leaving the disks, facet joints and osteoligamentous structures.

2) After the specimens were selected they were wrapped in saline soaked towels to protect them from dehydration and limit the deterioration of the soft tissue until testing could occur. C5, C4, and C3 vertebra were affixed with screws to each other to restrict their motion as illustrated in Figure 24. These caudal vertebras were solidified within a resin (see Figure 25), to a steel mounting plate while leaving the cranial end of the spine free to move when applied with a bending moment. The steel plate was mounted to a six-component load cell (Model MC3A-6-1000, AMTI Multi-component transducers, AMTI Inc., Newton, MA). The steel mounting plate was positioned at an approximate lordotic angle of 17 degrees. The vertebral bodies of C3, C4, and C5 were restricted as they were fixed indirectly yet solidly to the six axis load cell. The C2-C3 joint was not constrained. The motion of the C2-C3 joint allowed for the C1-C2 joint to translate with respect to the six axis load cell when applied with a bending moment. The maximum bending moment of plus/minus 1.5 Nm as recorded by the six axis load cell may have been slightly reduced at the C1-C2 joint due to its relative position with the applied load located at the end of the rods which produced the bending moment. The C2-C3 motion was not recorded but assumed to be consistent between testing of each specimen.

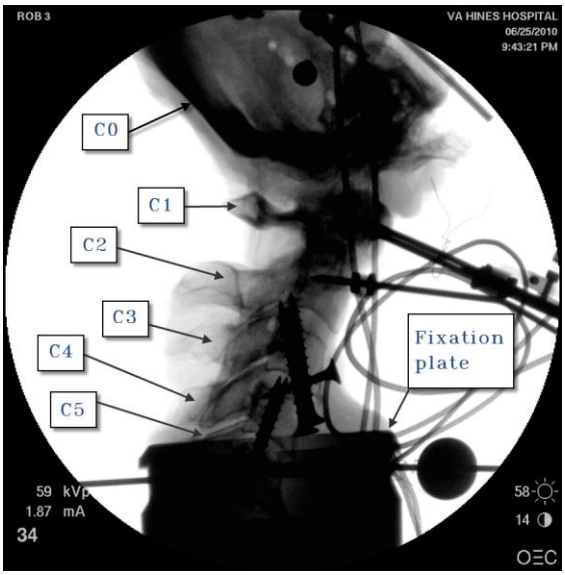

Figure 24. Fixation screws used at C3, C4, and C5 vertebra to limit motion.

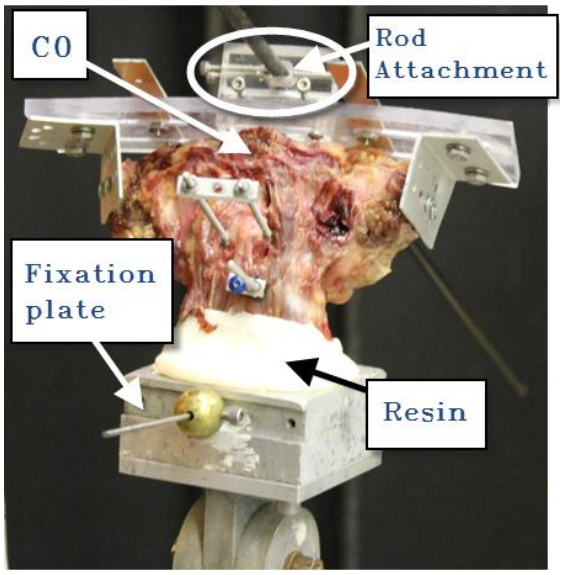

Figure 25. Resin applied to caudal vertebra to limit motion.

Flexion-Extension and Lateral Bending

3) The midpoint of a rod (bag offset length = 60 cm for FE and 46 cm for LB) was attached to C0, as illustrated in Figure 26 and Figure 27. This setup applied forces and moments to the cadaveric spines from water weight introduced from filling and un-filling bags attached to each end of the rod. The weight of this fixture was less than a two newtons which is less than that of a human head of approximately 29 N.[19] The midpoint of the fixture was located visually so it was posterior to the AA joint in the sagittal plane to provide some lordosis to simulate as close as possible sagittal balance. The two bags as illustrated in Figure 28 were filled and emptied in opposite cycles to provide an applied bending moment to the spine segment.

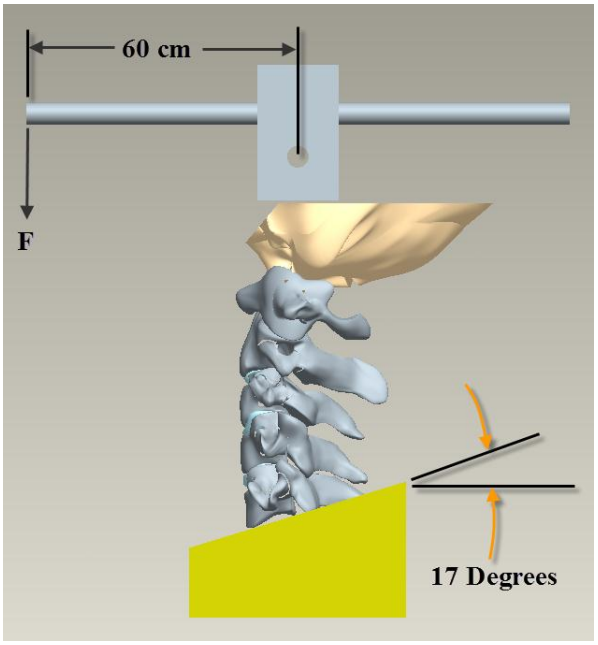

Figure 26. Flexion and Extension setup.

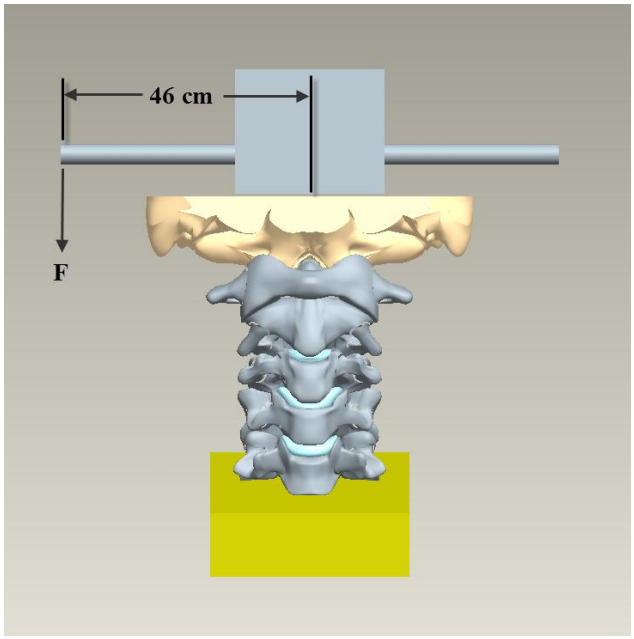

Figure 27. Lateral Bending setup.

4) A positive displacement pump system also pictured in Figure 28, allowed for continuous cycling of the specimens between a predetermined moment of plus/minus 1.5 Nm in FE, LB, and AR. The LB test setup can be seen in Figure 28. Three cycles for each type of motion were tested while collecting load-displacement data. The last two cycles were compared to ensure two reproducible cycles were obtained. The ranges of motion from these two cycles were averaged to determine the range of motion for each test. This type of test was previously performed at Patwarhan's lab and was reported due to the long moment arms (i.e. 60 mm and 48 mm) an off-axis moment was on average less than 0.1 Nm. As a result, no off-axis forces were analyzed in this test.[20]

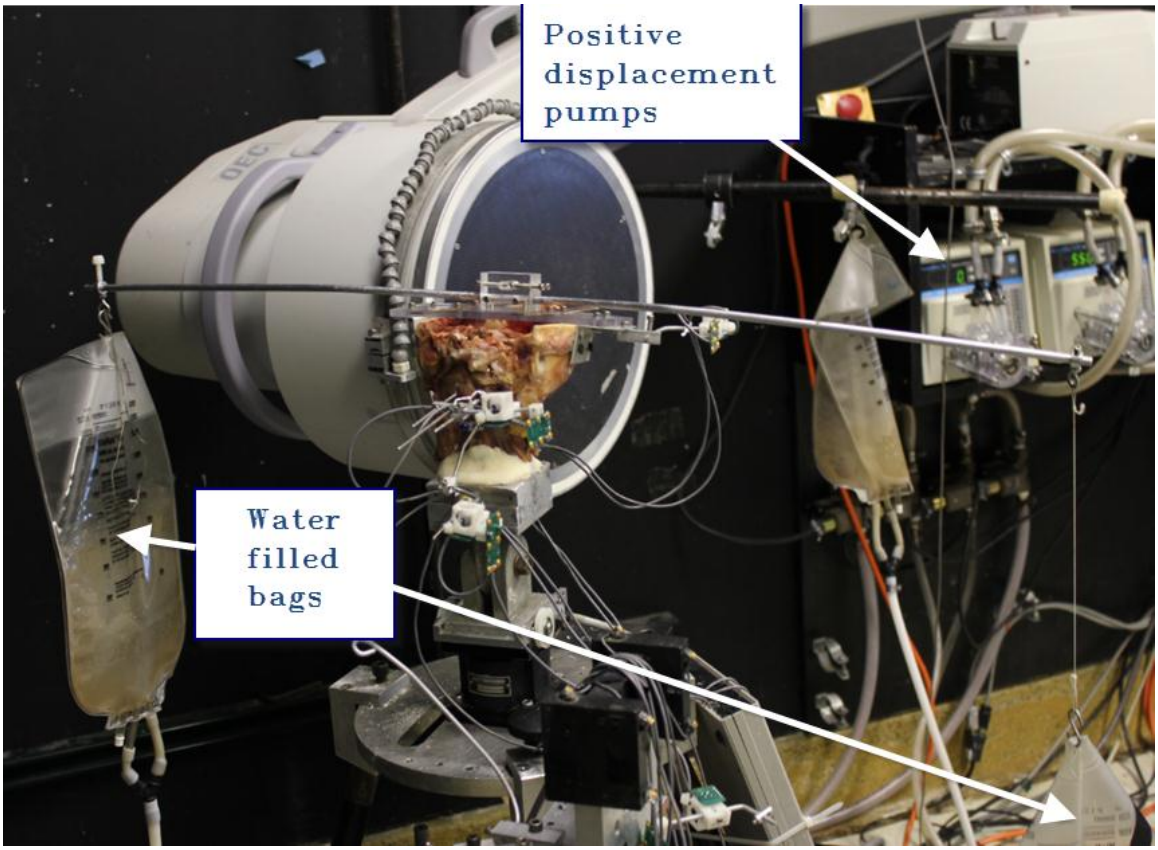

Figure 28. Lateral bending testing apparatus.

Axial Rotation

5) A cylinder was attached to C0 as illustrated in Figure 29. Two thin light weight cords were wrapped around the cylinder and an empty bag was attached to the ends of each cord, (i.e. 4 bags total). Water was distributed evenly between both the two F1 forces which results in a left to right shoulder motion or the two F2 forces which caused a right to left shoulder motion as pictured in Figure 30.

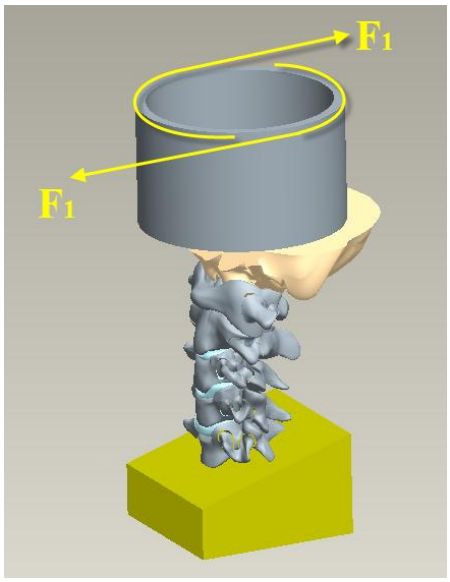

Figure 29. Illustration of AR setup (left to right shoulder motion).

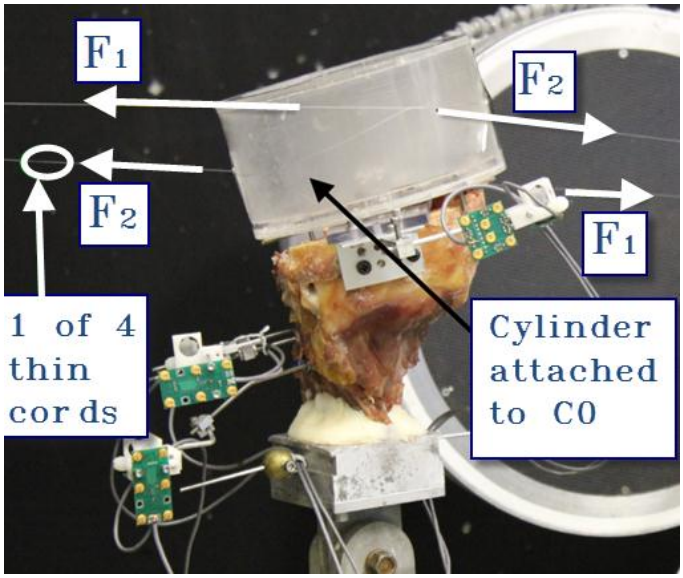

Figure 30. Illustration of AR of cadaveric spine.

6) Measurements of displacement were obtained using an optoelectronic motion measurement system, Model 3020, Optotrak®. In addition, a bi-axial angle sensor was mounted on each vertebra to verify results. Fluoroscopic imaging was used to view implant-vertebra motion. This instrumentation is shown in Figure 31.

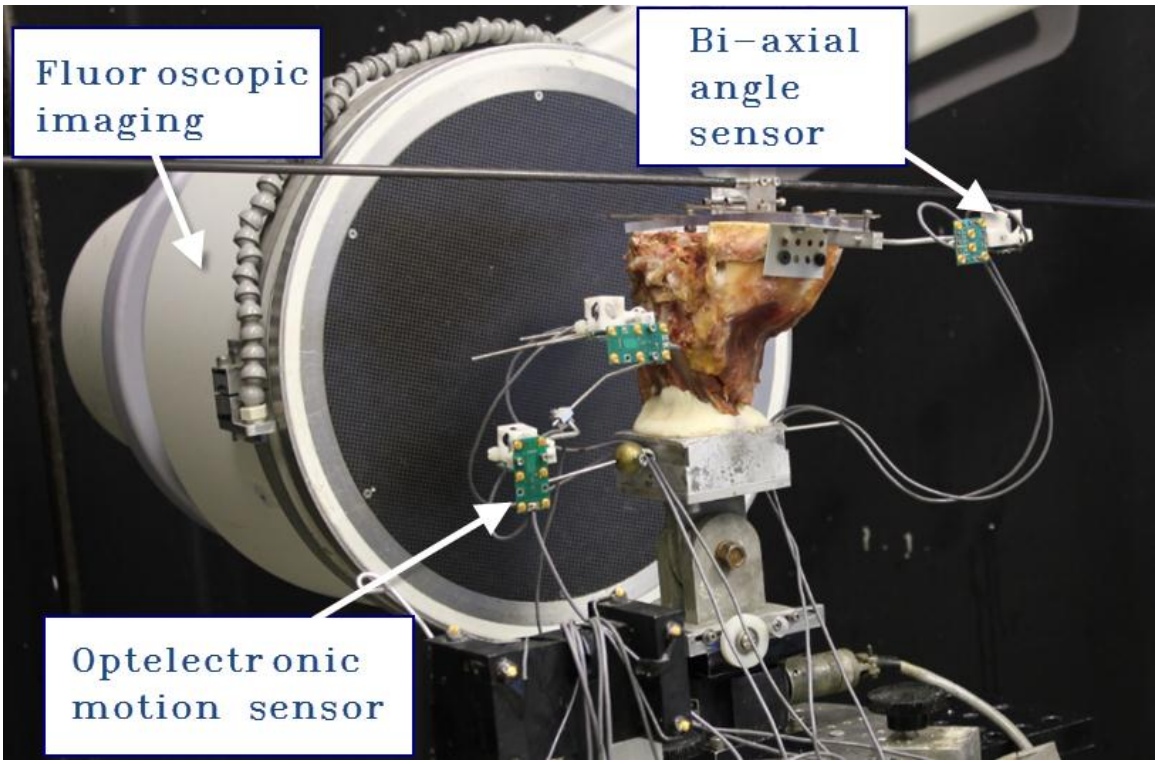

Figure 31. Measurement system.

7) The cadaveric spines were instrumented and tests conducted in the following order: Intact, destabilized with the BTS, destabilized with the Harms Technique, and finally destabilized without implants. Prior to breaking the odontoid, the BTS was attached and before removal of the BTS, the Harms construct was attached. This protocol provided the same vertebral relationship between tests. Finally, the destabilized spine was tested last.

8) Prior to implanting the BTS, the AA joint was observed as in Figure 32.

Figure 32. Observation of the Atlantoaxial joint.

9) Once the AA joint was located a partial capsule resection was performed. The AA joint was decorticated with a cob curette and the BTS was implanted as per Figure 33.

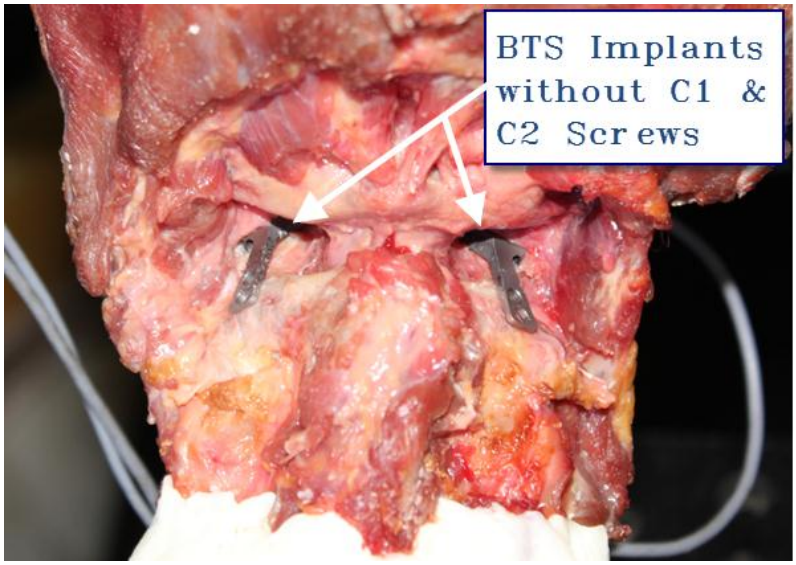

Figure 33. Implanted BTS.

10) After the BTS was situated, the C1 screw trajectory was drilled and tapped before insertion of the C1 Screw. Followed by drilling and insertion of the C2 screws (see Figure 34).

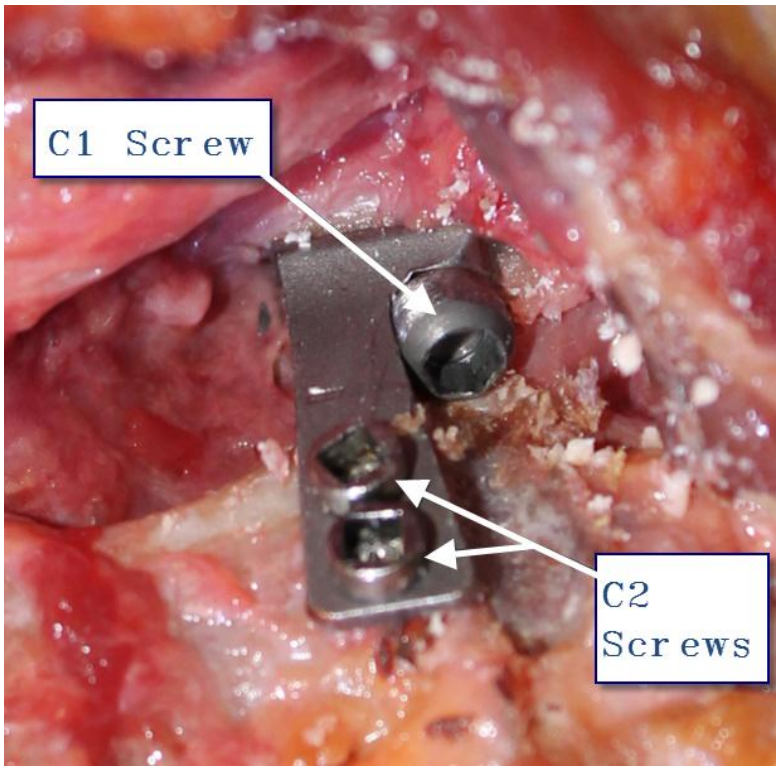

Figure 34. Implantation of C1 and C2 Screws.

11) The Harms technique instrumentation was attached and secured before the removal of the BTS implants in order to ensure the same anatomical positioning of the AA complex during testing. The C1 lateral mass screws and C2 pedical screws were placed as illustrated in Figure 35.

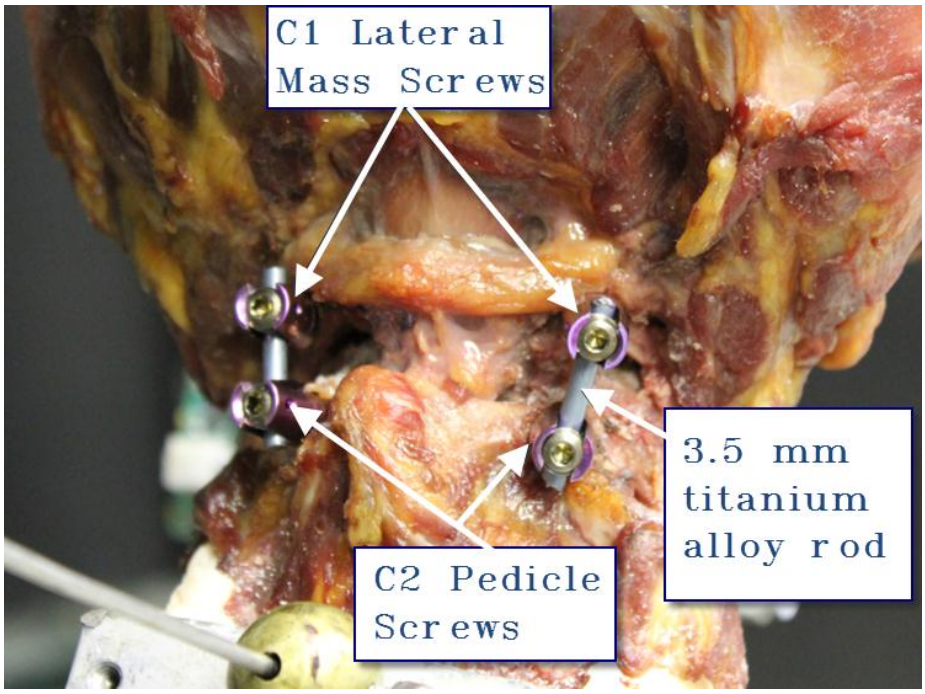

Figure 35. Harms Construct.

12) After testing of the Harms construct, the C1 lateral mass screws, C2 pedicle screws, and rods were removed. The spine was then tested to demonstrate the spine in the destabilized condition. This AAI condition consisted of a fractured odontoid process and the resection and alterations of the bilateral facet capsule due to insertion and removal of the BTS implant and Harms construct.

Statistical Computations

The change in angle between the C1 and C2 vertebra and the bending moment applied to a load cell connected with the test specimens are the two measurements collected by this study. The overall range of motion measured for each test was calculated from the motion limits during an applied +/- 1.5 Nm moment. The data collected was determined normal using an Anderson-Darling Normality test. Although a couple of individual tests

such as the AR and LB of the Harms with a broken odontoid indicated possible non-normality with p-value near 0.05. This could have been a result of the measured motion approaching very close to zero (physical one sided limit) which caused the data to skew or the limited sample size of 6 spines. This test method is a repeated measures test and a paired analysis could have been utilized to understand the impact to ROM due to the implantation of the BTS and Harms devices on spines with a broken odontoid. Such a repeated analysis is designed to remove the variations associated between specimens. Instead a different statistical method, one factor ANOVA, was used to analyzed the results and incorporate the spine variations. This approach address reduction of motion for the average spine motion tested instead of just reduction of each specimen's motion. Biomechanical analysis of the intact, BTS, Harms construct, and destabilized spine constructs (k=4 with n=6/each group) provided statistical evidence displayed in **Table 5**, which indicates that there was not a significant difference between the BTS and the Harms technique ($p > 0.1$). Because of the large reduction of motion between the destabilized condition and both the Harms and BTS, the statistical power is 1. The LB statistical power of these two devices to the destabilized condition is 0.78. The statistical power is low for the comparison between the Harms and BTS due to the small sample size, small difference between means relative to the standard deviation of the samples. The statistical power for comparing the BTS and Harms in FE, AR, and LB is 0.06, 0.08, and 0.5. relatively. The data collected were analyzed using a one factor ANOVA test as well as evaluating relationship variances between each group. The statistical data analysis in **Table 5** was performed using Systat 10.2 software package (Systat Software, Richmond, CA).

Table 5. Statistics (P-Values) for Flexion-Extension, Lateral Bending, and Axial Rotation Range of Motion

Atlanto-Axial Motion	BTS v. Destabilized	BTS vs. Harms
Flexion-Extension	0.00007	1.00
Axial Rotation	0.006	0.15
Lateral Bending	0.0003	1.00

Results

The Optoelectronic motion measurement system contributed an estimated +/- 0.25 degree error to the recorded angle recorded. Two measured test results reflected a negative range of motion: (Specimen #8, Harms, AR= -0.3 and Specimen #8, BTS, LB= -0.04). Since these tests have a minimum physical limit of zero, then the combined instrument error and method must have at least an overall test error of +/- 0.4 degrees to explain a negative test ROM. The results provided statistical evidence ($p < 0.01$) to support a reduction of C1-C2 motion when instrumented with either the Harm's technique or the BTS device in FE and AR associated with the torsion load of 1.5 Nm as compared to the destabilized condition. The BTS and Harms techniques also demonstrated a significant difference ($p < 0.01$) in comparison with the intact spine in FE and AR. Intact Spine motion in FE and AR for the AA joint demonstrated a range of motion of 14°, sd = 3° and 67°, sd = 14°, respectively. After implantation of the BTS these two motions were reduced to FE of 4°, sd = 2° and AR of 1°, sd = 1°. A significant change in motion was not demonstrated in LB. Intact motion was measured at 2°, sd = 1°. With the BTS and Harms the LB motion was measured at 0°, sd = 1°; 1°, sd = 1°, respectively. One contributing factor to the inability to measure comparable differences with the intact LB motion was the large ratio of test results producing large values of statistical variance as

compared to mean. The LB test did not have a significant difference in variance ($p > 0.1$) than FE or AR. The AA LB intact joint provides very limited intact motion, and as a result, this statistical test, either due to test method errors or consistency in C1-C2 motion, provided for too great a variance to demonstrate a reduction in motion. No significant difference between the Harms and BTS instrumentation was detected (CI = 99%) in all six degrees of freedom (FE, LB, and AR).

Discussion

The next three figures show the FE, AR, and LB load vs. position curves that were collected using Specimen #3. This specimen was chosen for illustration purposes because it represents a typical response of the atlanto axial joint as a result of the applied loads used in this study. In Figure 36, Figure 37, and Figure **38** the x-axis represents the applied moment transferred to the AA motion segment and the relative angle changes are reflected by the y-axis. The angles are not absolute values but are relative measurements. The data are relative to pairs of the physical sensors as they were mounted on the vertebral bodies. The angle measurements do not represent the endplate angles. At the ends of each s-curve as the applied moment approaches either 1.5 Nm or -1.5 Nm the slope decreases as ligaments stretch to their extremes. An asymptotic curve is observed near the hyper limits of motion and is a result of the viscoelastic characteristics of the ligament. [21] These limits create the ROM for the atlanto axial joint. (Surgery1 = BTS, Surgery 2 = Harms, and Surgery 3 = Destabilized)

C1-C2 F/E Moment-Angle Curve

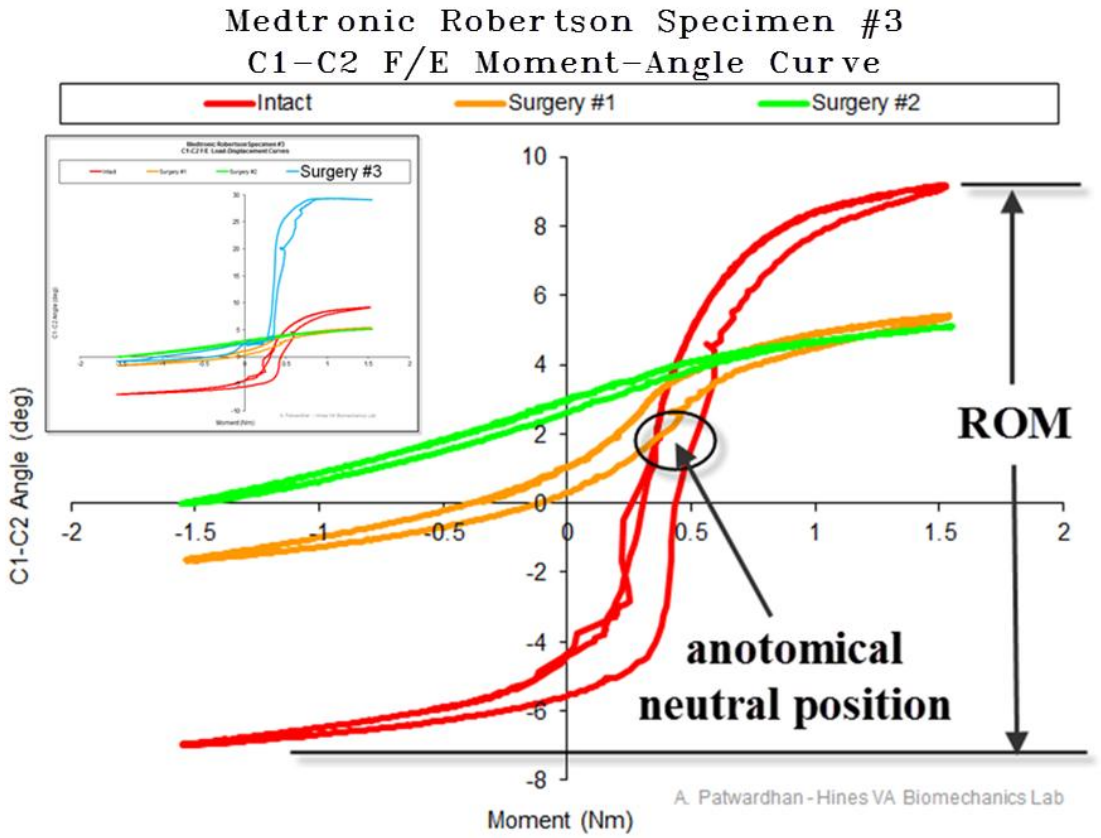

Figure 36. Specimen #3 Flexion and Extension motion.

A graphical representation of the FE motion, induced in Specimen #3, as a result of the 1.5 Nm moments in the sagittal plane is shown in Figure 36. The cadaveric spines were affixed to the load cell to model as closely as possible anatomical sagittal balance. The associated C0-C3 vertebras created a lordotic curve due to their anatomical shapes and attachment of the fixtures to produce the loading scenarios. The non-zero bending moment location of the "anatomical neutral position" label from Figure 36 is a result of the attachment of the instrumentation that applied the load, the angle of attachment of the lowest fixed vertebral bodies, and the weight of the anatomy of the spine cranial to the

C1-C2 joint. The data reflects FE curves with asymptotic ends near the plus/minus 1.5 Nm loads which indicates that the test setup does capture the full motion of the C1-C2 joint. The X-axis location of the intact "anatomical position" of this joint for this test is incidental to the measurement of the change in overall range of motion between each of the tested conditions. The affixed angle between C1 and C2 was not measured after surgery 1 and 2. This fixed position was decided by Dr. Robertson during surgery 1 as determined by his judgment to restore sagittal balance. This study did not measure the performance of surgery 1 and surgery 2 with respect to flexion vs. extension, but only compared the overall range of motion after surgeries 1 and 2. The positive X-axis location of the "anatomical neutral position" as reflected in Figure 36 illustrates that the C1-C2 joint position was somewhat lordotic due to posterior load as created by the test setup as described in the methods section.

The motion curve for each, (intact, BTS, Harms, and destabilized), consisted of two s-curves separated by a space. The bottom s-curve is the spine in flexion and the top s-curve represents an extension motion. The area within the FE curves, near the midpoint between the extreme limits of the ROM creates a hysteresis which represents the typical area for anatomical motion. The ideal angular position of the AA joint for the least amount of ligament stretch and musculature contribution in the sagittal plane occurs when the center of the ROM is at zero bending moment. This does not occur in erect human posture because the center of gravity of the head is typically positioned posterior to the C1-C2 vertebral joint. This specimen as mounted requires a flexure force of approximately 0.4 Nm to maintain a steady state AA joint in the neutral position. The

range of motion of specimen 3# created by both the BTS and Harms both decreases the range of motion compared to the intact condition as illustrated (Figure 36).

C1-C2 AR Moment-Angle Curve

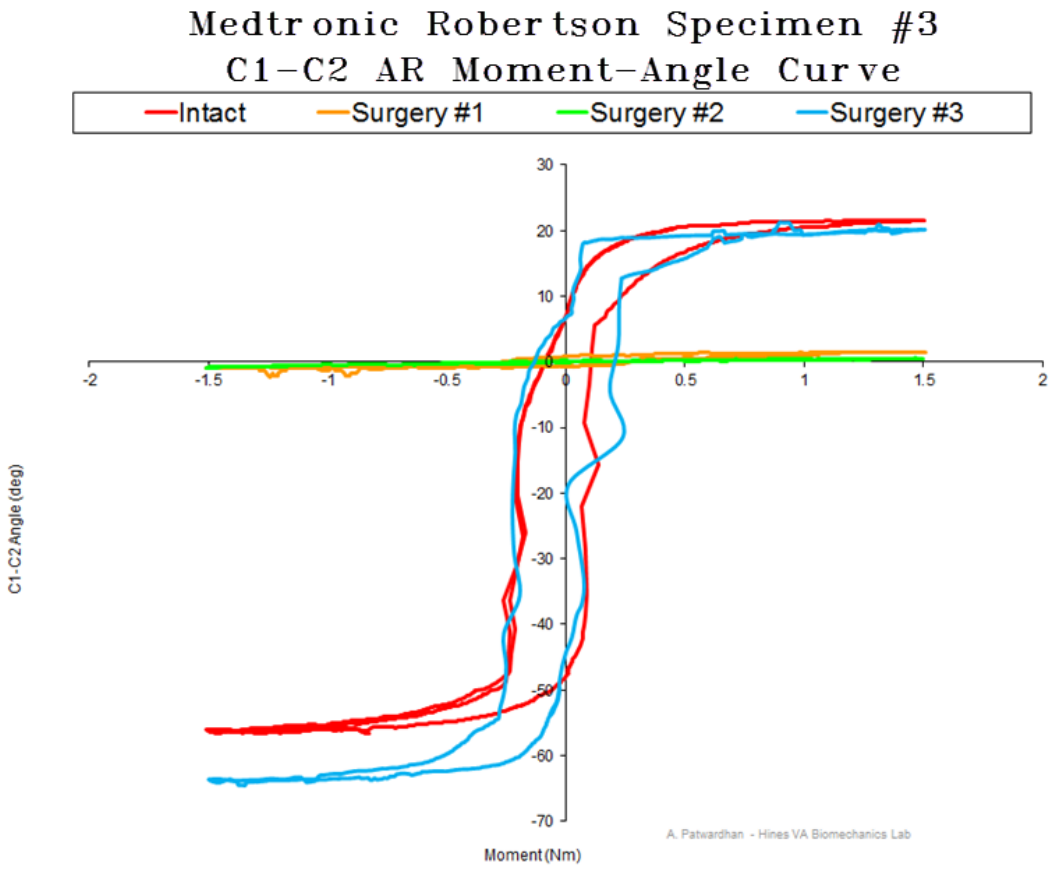

Figure 37. Specimen #3 Axial Rotation motion.

A graphical representation of the AR motion in Specimen #3 induced as a result of the ±1.5 Nm moments occurring in the axial plane is illustrated in Figure 37. Two curves, (intact and destabilized) consist of two s-curves separated by a space. The bottom s-curve is the spine in left to right shoulder rotation and the top s-curve represents right to

left shoulder rotation. The area within the AR curves, near the midpoint between the extreme limits of ROM creates a hysteresis which represents the ideal area for anatomical motion. Consistent with other published studies, the AR motion is the predominant motion of the atlanto axial joint. The type-2 odontoid fracture destroyed the ability of the apical and alar ligament to restrict motion but did not dramatic affect AAI in AR as it did in flexion extension (AR intact = 67.3 ± 13.8 Nm and AR destabilized = 74.2 ± 16.1 Nm). This constitutes only a 10% increase in AR vs. 124% increase in FE. The curves for surgery 1 and surgery 2 illustrate very little change in angle over the applied ±1.5 Nm moment. As a result, AR ROM decreases significantly when either the BTS or Harms surgical technique is performed.

The location of the data with respect to the Y-axis is not related to other specimens or test setup because the angle of the joint is relative only to its specific curve and is not absolute. The intact curve reflected in Figure 37 is more symmetrical to a zero moment of the X-axis than the FE curves. This is because the spine is more symmetrical in the coronal plane and the fixtures were intentionally mounted symmetrical to the spine in the coronal plane. As a result, the middle of the "anatomical position" is near the zero position of the X-axis.

C1-C2 LB Moment-Angle Curve

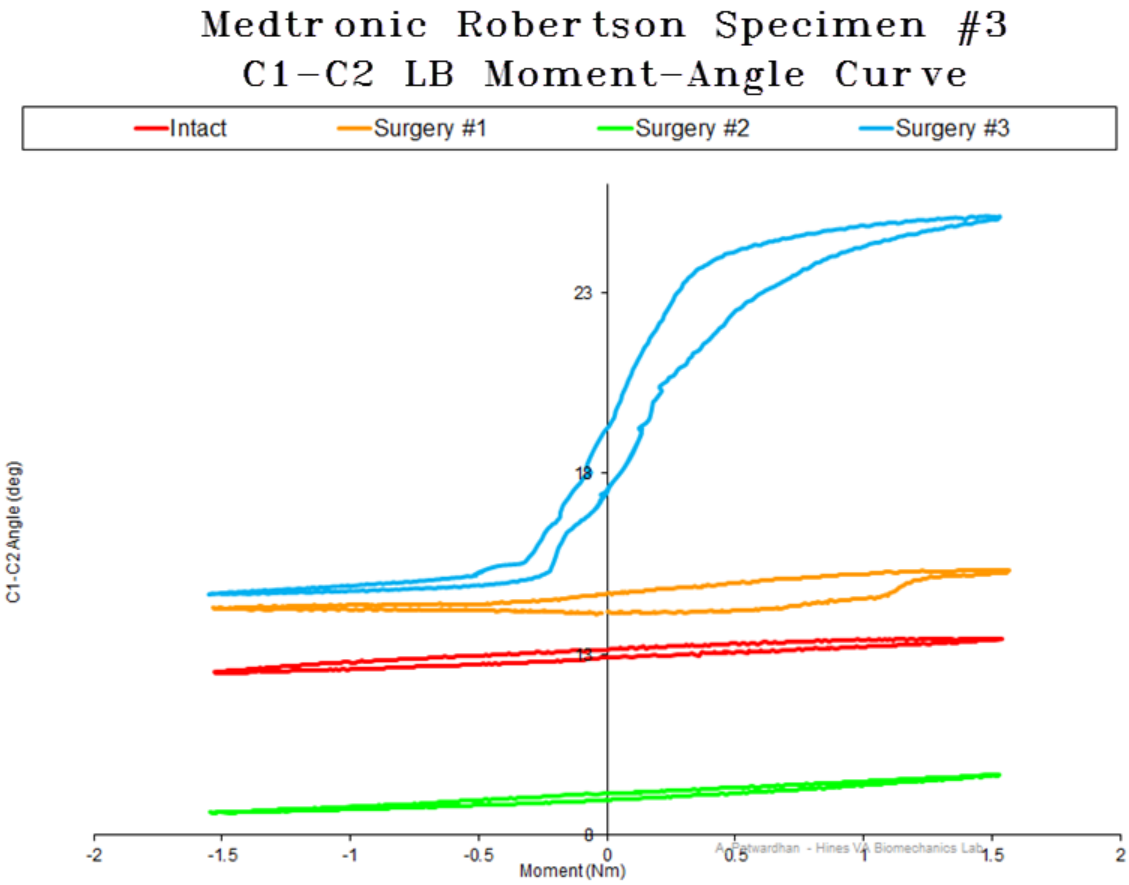

Figure 38. Specimen #3 Lateral Bending motion.

A graphical representation of the LB motion for Specimen #3 induced as a result of the ±1.5 Nm moments occurring in the coronal plane is illustrated in Figure 38. This intact joint contributes the least motion in LB (4° ± 3°) between the three studies of motions. This joint was the most affected in the destabilized condition as a result of surgery #3 and increased in motion by an average of 480% as compared to the intact condition. The variation in the Y-axis positions between each of these surgeries is because the data are relative and not absolute. The data are reflected as collected. Between surgeries the

sensors can be touched slightly and provide the shift between surgeries. The important information is the overall range of motion for each surgery not the relative position along the Y-axis which is relative and not absolute.

Flexion Extension Range of Motion

Individual specimen results are provided in appendix A as shown in Figure 39. Intact spine motion in FE of C1-C2 demonstrated a range of motion of 14, sd = 3 degrees. After implantation of the BTS these two motions were reduced to 4, sd = 2 degrees. The Harms technique resulted in a reduction also, to 4, sd = 2 degrees. Both the BTS and Harms technique after instrumented demonstrated a significant difference in motion. ($p < 0.01$) as compared to the destabilized condition.

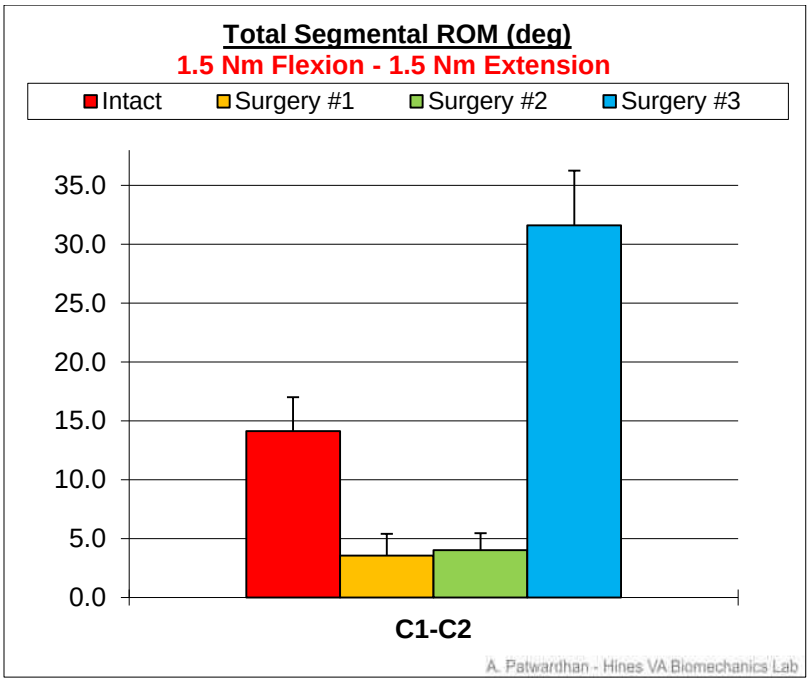

Figure 39 Flexion Extension test results (k=4, n=6).

Flexion Extension Scatter Plot

This scatter plot, Figure 41, reveals that both intact specimen #7 and #8 are substantially less than the rest of the measured results. Although they appear to be outliers when compared to the results from Dr. Dvorak's previous intact ROM located in Table 1, they are not substantially different than could be expected. ($p > 0.01$) The scatter plot reveals possible outliers for both the BTS and Harms. Since they appear on different specimens it is assumed to be the variation in surgical consistency in implantation. As a result, they are not removed from the FE statistical analysis.

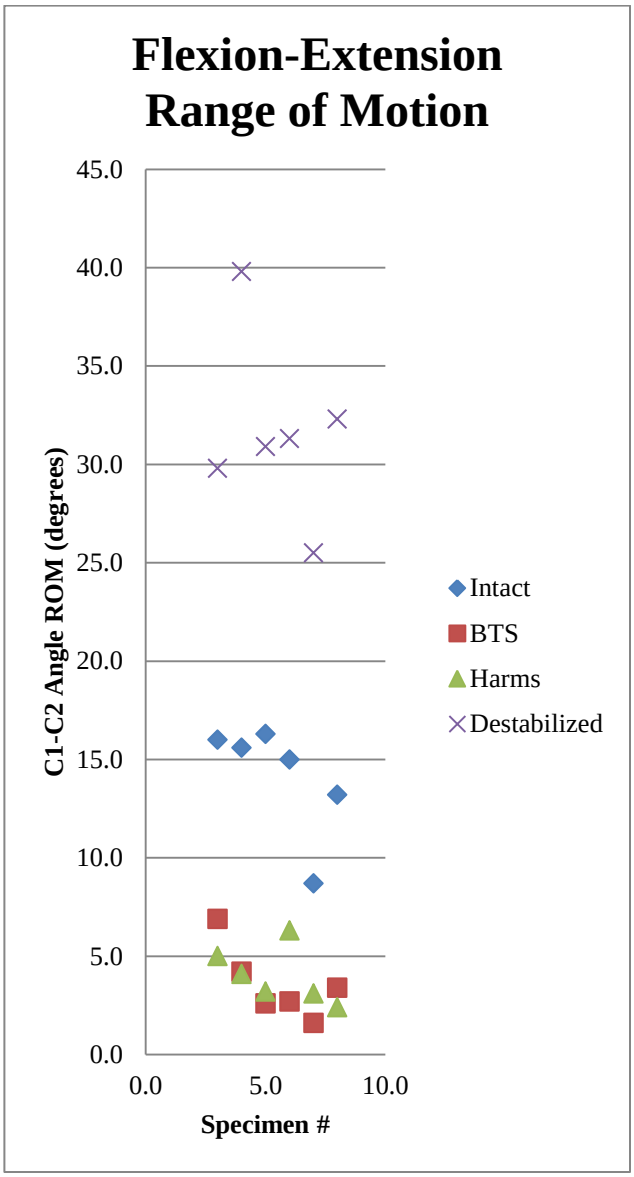

Figure 40. Flexion-Extension Scatter Plot of Results.

Axial Rotation Range of Motion

The ROM for AR is illustrated in Figure 41. Individual specimen results are provided in appendix A. Intact spine motion in AR for C1-C2 demonstrated a range of motion of 67, sd = 14 degrees. After implantation of the BTS the AR motion was reduced to 01, sd = 1 degrees. The Harms technique resulted in a reduction also to 1, sd = 1 degrees. Both the BTS and Harms technique after instrumented demonstrated a significant difference in motion. ($p < 0.01$)

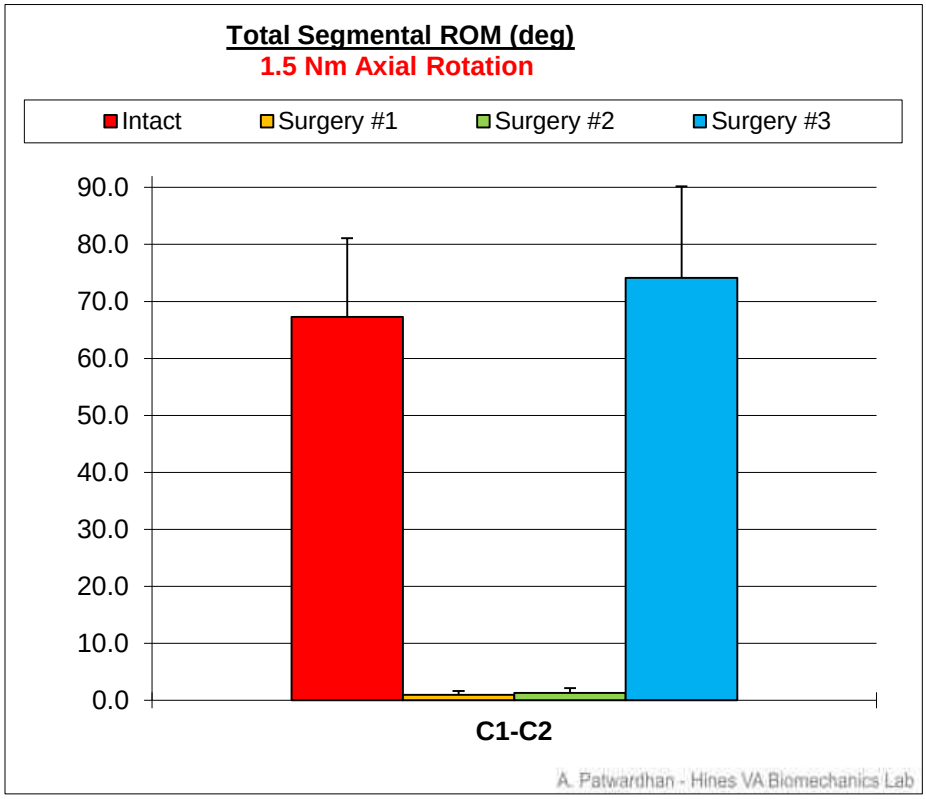

Figure 41. Axial Rotation test results (k=4, n=6).

Axial Rotation Scatter Plot

The ROM for each specimen in AR is illustrated in Figure 42. This scatter plot reveals that both intact specimen #7 and #8 are substantially less than the rest of the measured results. Although they appear to be outliers when compared to the results from Dr. Dvorak's previous intact ROM located in Table 1, they are not substantially different than could be expected. ($p > 0.01$) The AR scatter plot does not reveal any outliers for either the BTS or Harms technique. As a result, all the specimens are used in the AR statistical analysis.

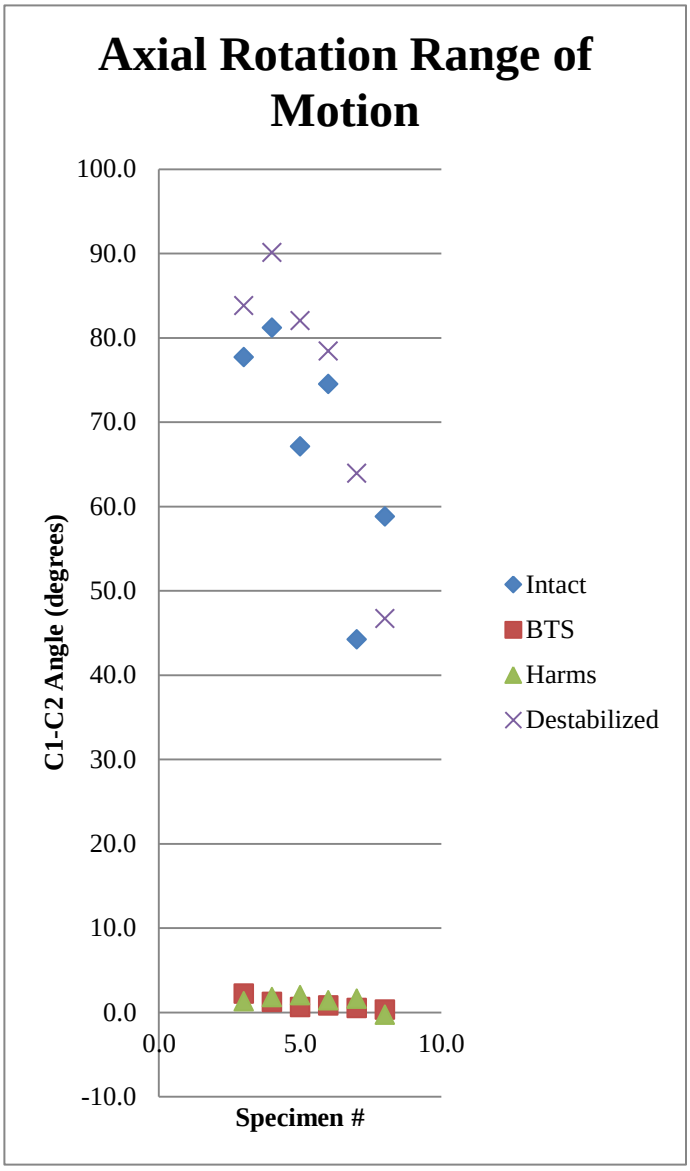

Figure 42. Axial Rotation Scatter Plot of Results.

.

Lateral Bending Range of Motion

The ROM for LB is illustrated in Figure 43. Individual specimen results are provided in appendix A. Intact motion was measured at 1.8, sd = 1.1 degrees. With the BTS the LB motion was measured at 0, sd = 1 degrees. The Harms technique also resulted in a reduction in motion to 1, sd = 1 degrees. Both fixation devices provided a significant reduction in lateral bending in relationship with the destabilized model, Surgery 3. A significant change in motion compared with intact was not demonstrated in LB due to either the BTS or Harms instrumentation. This may be because this joint provides very limited intact spine motion in lateral bending (LB).

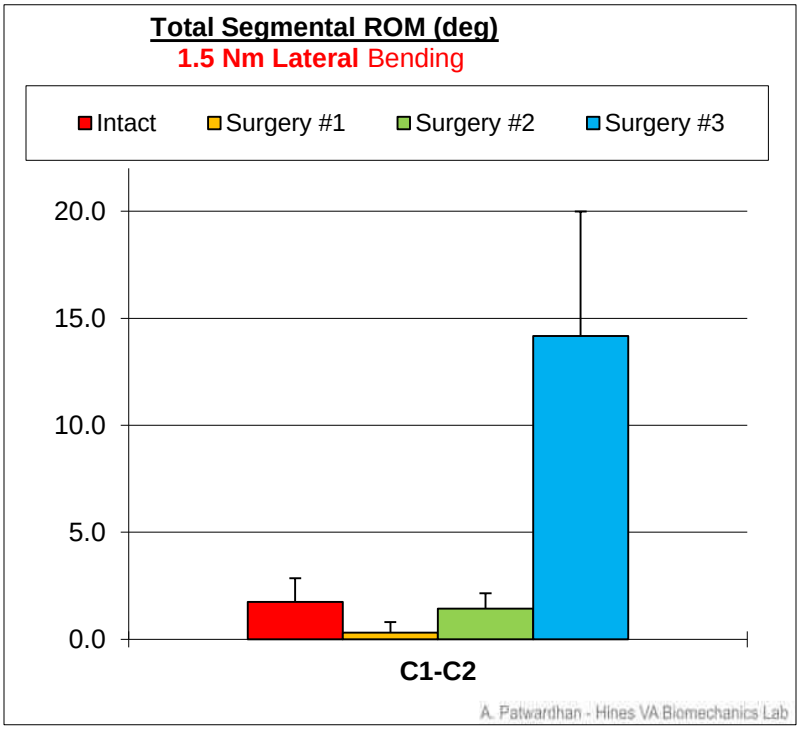

Figure 43. Lateral Bending test results (k=4, n=6).

Lateral Bending Scatter Plot

The ROM for each specimen in LB is illustrated in Figure 44This table demonstrates the magnitude difference in destabilized ROM variances compared to intact, BTS, and Harms. To provide a graphical representation of the ROM variations between specimens for intact, BTS and Harms Figure 45 is provided. This chart illustrates that the test results for LB does not provide any significant difference between Intact, BTS, and Harms due to the large measured variances in the individual test results. The BTS result from Specimen #7 indicated a negative angle. This was a result of a true motion approaching zero minus the measurement error.

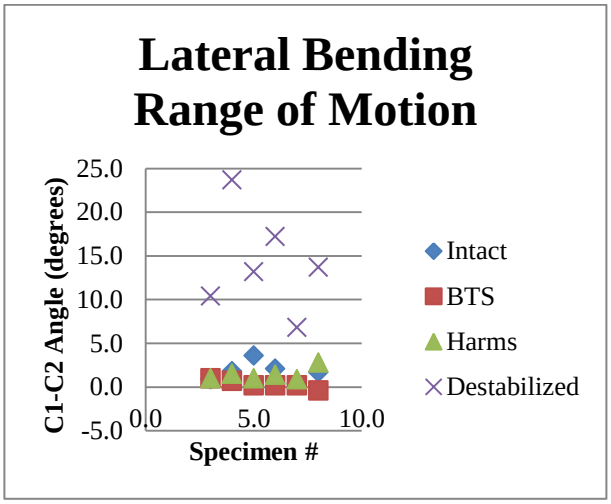

Figure 44. Lateral Bending Scatter Plot of Results.

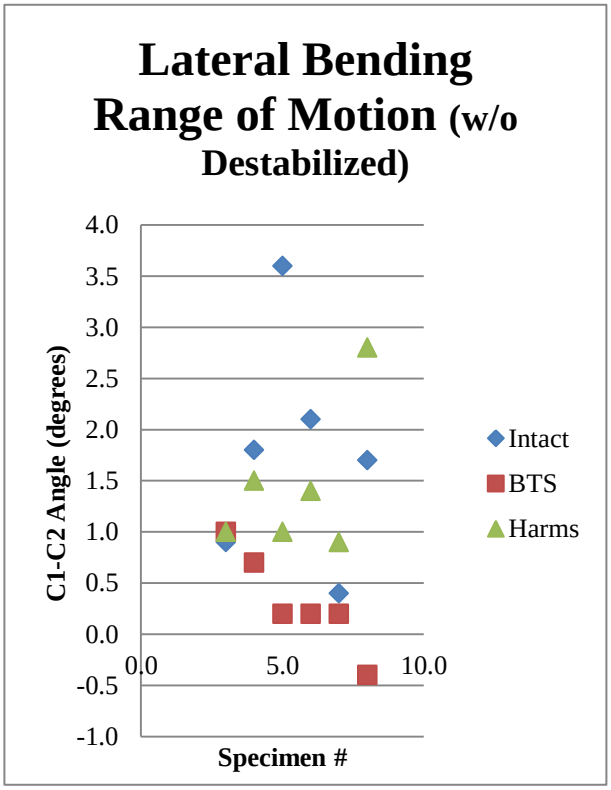

Figure 45 Lateral Bending Scatter Plot of Results (without Destabilized).

Surgical Technique

In addition to the biomechanical testing conducted, three BTS surgical technique labs were performed with Dr. Robertson to confirm if an improved surgical technique was achievable. In December 2010, a cadaver lab was conducted at the MERI in Memphis, TN using the same implant design as tested at Patwardhan's lab. During this lab it was determined that the posterior-to-anterior C1 screw trajectory, which converges in the axial plan as illustrated in Figure 46, results in traversing the VAF as pictured in Figure 47 in this specimen.

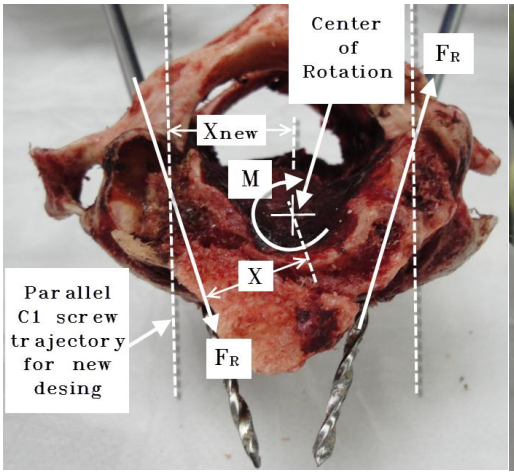

Figure 46. Inferior view of C2 Vertebra illustrating C1 screw trajectory in the axial plane.

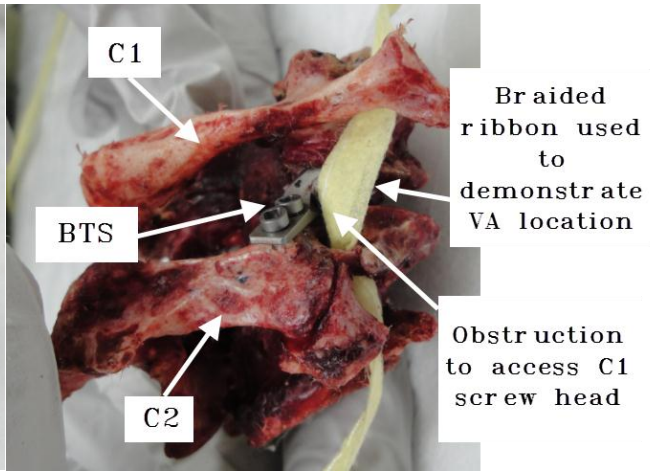

Figure 47. Illustration of C1-C2 corpectomy with VA obstruction of C2 screw trajectory.

As a result of these labs, it was determined that future BTS designs needed to be implanted with the C1 screw trajectory parallel to the sagittal plane and centered over the C1-C2 Lateral mass region as illustrated in Figure 6. This trajectory provides a clear access for drilling, tapping, and screw placement. This change in C1 screw trajectory will slightly increase the distance (X) as illustrated in Figure 46. This straight trajectory

should also improve FE stabilization because the screws will be placed perpendicular to the FE motion. It was confirmed that the direct posterior approach allows for visibility of the AA joint and exiting nerve root during implantation of the BTS as illustrated in Figure 48. It was confirmed that the BTS flange is narrow enough to be located on the C2 lamina without impacting the spinal cord foreman.

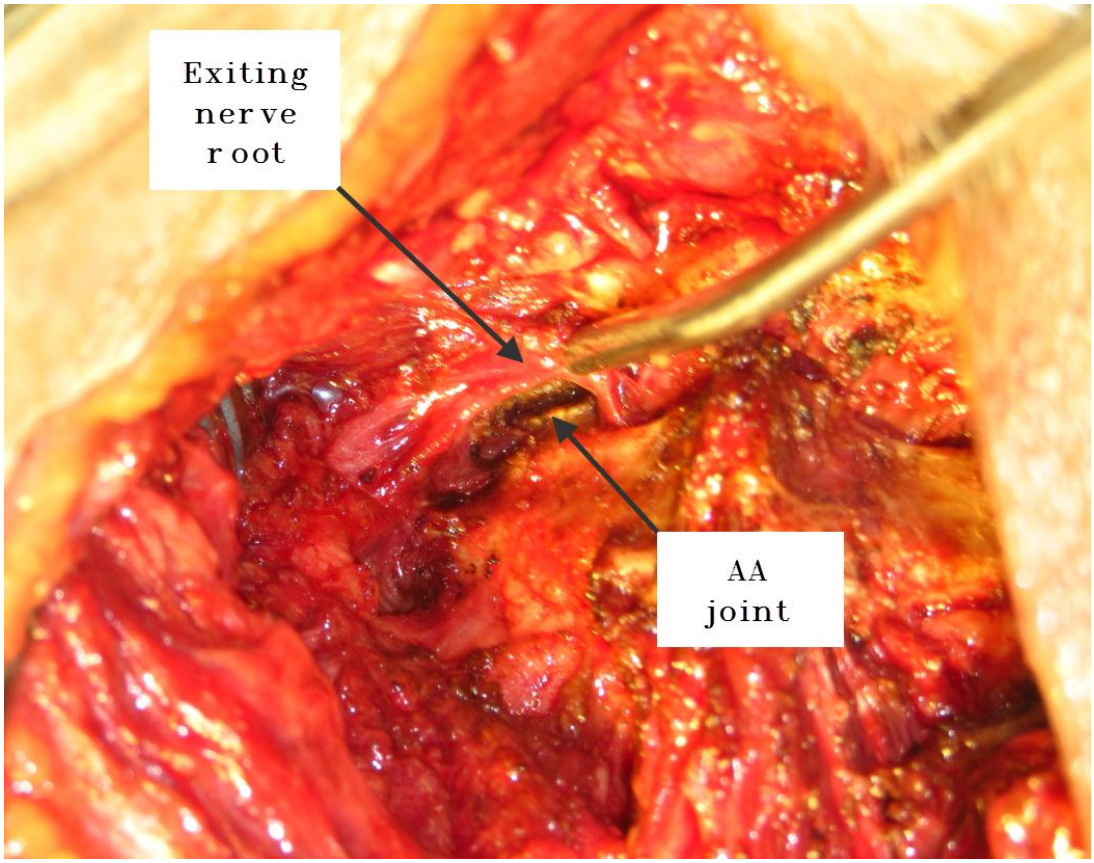

Figure 48. BTS posterior surgical approach.

Study Limitations

This study has limitations such as sample size, loading conditions, test setup, and order of testing. Approximately two newtons of offset loads were applied by the fixtures which were not analyzed for their location or contribution to offset axial loading to the spine. The contribution of the axial load was not evaluated in this experimental setup and assumed consistent between surgeries. The bending moments applied as well as the offset loads were small and do not simulate the clinical loads that could be experienced by the weight of the human head after such a device is implanted. There are several other conditions not measured by this test set-up that would provide a greater understanding in the performance of the BTS, such as the translation of the AA joint during the FE, LB, and AR tests. Also, measuring the performance of the BTS vs. the Harms device at loading conditions to cause mechanical failure of these devices were not tested. It was assumed that the measured range of motion of the destabilized spine, which was tested last due to concerns of losing sagittal alignment of the spine between surgeries, would have been the same if tested prior to testing of the BTS with a broken odontoid and testing the Harms with a broken odointoid. Another limitation of this test is that the Harms device was tested after the BTS device. This order was necessary because the C2 Harms screws were much larger than the C2 BTS screws. If the C2 Harms screws were located and removed before placement of the C2 BTS screws, the resultant bone quality would have been dramatically deminshed for the C2 BTS screws. Due to the size of the C2 Harms screw and the depth of bone purchase within the the C2 vertebra, it was assumed that placing the C2 BTS screws first did not decrease the stability of the Harms device.

Conclusions

In conclusion, the testing performed provides evidence for the initial feasibility of the new BTS device as a means to stabilize the AA joint similarly to the Harms technique when loads of +/- 1.5 Nm are applied in FE, LB and AR. This device demonstrated a statistical reduction in AR, FE, and LB to the destabilized spine ($p < 0.1$) (appendix B). Some design changes in the BTS have been identified such as the C1 screw trajectory. With these changes the BTS can provide a safe surgical approach to minimize impact of the VAF, spinal cord, and C1 exiting nerve root.

References

1. White AA, Panjabi MM. *Clinical Biomechanics of the Spine*. 2nd ed. Philadelphia: Lippincott Williams and Wilkins; 1990.
2. Schnuerer, AP, Gallego, JM. *Basic Anatomy & Pathology of the Spine.* Memphis: Medtronic. 1998
3. Bahadurl R, Goyal T, Dhatt S, Tripathy SK. Transarticular screw fixation for atlantoaxial. *Journal of Orthopaedic Surgery and Research* 2010;5:1-8.
4. Schulz R, Macchiavello N, Fernandez E, et al. Harms C1–C2 Instrumentation Technique. *Spine* 2011;36(12):945–50.
5. Hartl R, Chamberlain RH, Fifield MS, et al. Biomechanical comparison of two new atlantoaxial fixation techniques with C1–2 transarticular screw-graft fixation. *J Neurosurg Spine* 2006;5:336–42.
6. Patwardhan AG, Havey RM. Load-carrying capacity of the human cervical spine in compression is increased under a follower load. *Spine* 2000;25:1548-54.
7. Henriques T, Cunningham BW, Olerud C, et al. Biomechanical comparison of five different atlantoaxial posterior fixation techniques. *Spine* 2000;25: 2877–83.
8. Melcher RP, Puttlitz CM, Kleinstueck FS, et al. Biomechanical testing of posterior atlantoaxial fixation techniques. *Spine* 2002;27:2435–40.
9. Uribe JS, Ramos E, Youssef AS, et al. Craniocervical Fixation With Occipital Condyle Screws. *Spine* 2010;35:931–8.
10. Dmitriev AE, Lehman RA, Helgeson, MD, Sasso RC, Kuhns C, Riew DK. Acute and Long-term Stability of Atlantoaxial Fixation Methods. *Spine* 2009;34:365–70.
11. Kelly BP, Glaser JA, DiAngelo DJ. Biomechanical Comparison of a Novel C1 Posterior Locking Plate With the Harms Technique in A C1-C2 Fixation Model. *Spine* 2008;33:920–5.

12. Oda I, Abumi K, Sell LC, Haggerty CJ, Cunningham BW, McAfee PC. Biomechanical Evaluation of Five Different Occipito-Atlanto-Axial Fixation Techniques. *Spine* 1999;24:2377–82.
13. Goel A. Atlantoaxial joint jamming as a treatment for atlantoaxial dislocation: a preliminary report. Technical note. *J Neurosurg Spine* 2007;7:90–4.
14. Dvorak J, Froehlich D, Baumgarthner H, Panjabi, MM. Functional radiographic diagnosis of the cervical spine: flexion/extension. *Spine* 1988;13:748-55.
15. Panjabi MM, Dvorak J, Duranceau J, et al. Three-dimensional movements of the upper cervical spine. *Spine* 1988;13:726–30.
16. Gallie W. Fractures and dislocations of the cervical spine. *Am J Surg* 1939;46:495–9.
17. Robertson PA, Tsitsopoulos PP, Voronov LI, Havey RM, Patwardhan AG. Biomechanical investigation of a novel integrated device for intra-articular stabilization of the C1–C2 (atlantoaxial) joint (2012). Spine;12:136-142.
18. Harms J, Melcher PR. Posterior C1–C2 fusion with polyaxial screw and rod fixation. *Spine* 2001;26:2467–71.
19. Echarri JJ, Forriol F. (). Influence of the type of load on the cervical spine: a study on Congolese bearers. *Spine* 2005;5:291-6.
20. Patwardhan AG, Tzermiadianos MN, Tsitsopoulos PP, et al. Primary and coupled motions after cervical total disc replacement using a compressible six-degree-of-freedom prosthesis. *European Spine Journal* 2010;DOI: 10.1007/s00586-010-1575-7
21. Möller J, Nolte L, Visarius H, Willburger R, Crisco J, Panjabi M. Viscoelasticity of the alar and transverse ligaments. *European Spine* 1992:1:178-84.

APPENDIX A: CADAVER TEST RESULTS (SPECIMENS 3-8)

Flexion-Extension Range of Motion:

C1-C2	Intact	BTS	Harms	Destabilized
3	16	6.9	5	29.8
4	15.6	4.2	4.1	39.8
5	16.3	2.6	3.2	30.9
6	15	2.7	6.3	31.3
7	8.7	1.6	3.1	25.5
8	13.2	3.4	2.4	32.3
AVG	14.1	3.6	4	31.6
sd	2.9	1.8	1.4	4.6

Axial Rotation Range of Motion:

C1-C2	Intact	BTS	Harms	Destabilized
3	77.7	2.2	1.3	83.8
4	81.2	1.2	1.8	90.1
5	67.1	0.6	2	82
6	74.5	0.8	1.4	78.4
7	44.2	0.5	1.6	63.9
8	58.8	0.3	-0.3	46.7
AVG	67.3	0.9	1.3	74.2
sd	13.8	0.7	0.8	16.1

Lateral Bending Range of Motion:

C1-C2	Intact	BTS	Harms	Destabilized
3	0.9	1	1	10.4
4	1.8	0.7	1.5	23.7
5	3.6	0.2	1	13.2
6	2.1	0.2	1.4	17.2
7	0.4	0.2	0.9	6.8
8	1.7	-0.4	2.8	13.7
AVG	1.8	0.3	1.4	14.1
sd	1.1	0.5	0.7	5.8

APPENDIX B: ONE FACTOR ANOVA ANALYSIS

Flexion-Extension

	intact		Surgery 1		Surgery 2		Surgery 3
n=	6	n=	6	n=	6	n=	6
mean=	14.10	mean=	3.60	mean=	4.00	mean=	31.60
Sa^2=	8.41	Sb^2=	3.24	Sc^2=	1.96	Sc^2=	21.16
sd=	2.90	sd=	1.80	sd=	1.40	sd=	4.60

		F_{test} or	
alpha=	0.01	VR=	118.75
K=	4	$F_{(0.90,3,20)}$=	2.38
N=	24	$F_{(0.95,3,20)}$=	3.10
X=	13.33	$F_{(0.99,3,20)}$=	4.94
Sb^2=	1032.22	since VR> Fcritical, we reject the null and	
Sw^2=	8.69	accept the alternative because p<0.01	

Bonferroni - two tailed

(alpha/4)= 0.0025

$t_{critical\ (20,.0025)}$= 5.60

compare intact with surgery 1 (BTS)
t= 6.17

compare intact with surgery 2 (HARMS)
t= 5.93

compare intact with surgery 3 (destabilized)
t= -10.28

compare surgery 1 (BTS) with surgery 2 (HARMS)
t= -0.23

compare surgery 1 (BTS) with surgery 3 (destabilized)
t= -16.45

compare surgery 2 (HARMS) with surgery 3 (destabilized)
t= -16.21

Beyond $F_{critical}$

Axial Rotation

	intact		Surgery 1		Surgery 2		Surgery 3
n=	6	n=	6	n=	6	n=	6
mean=	14.10	mean=	3.60	mean=	4.00	mean=	31.60
Sa^2=	8.41	Sb^2=	3.24	Sc^2=	1.96	Sc^2=	21.16
sd=	2.90	sd=	1.80	sd=	1.40	sd=	4.60

		F_{test} or	
alpha=	0.01	VR=	118.75
K=	4	$F_{(0.90,3,20)}$=	2.38
N=	24	$F_{(0.95,3,20)}$=	3.10
X=	13.33	$F_{(0.99,3,20)}$=	4.94
Sb^2=	1032.22	since VR> Fcritical, we reject the null and	
Sw^2=	8.69	accept the alternative because p<0.01	

Bonferroni - two tailed

(alpha/4)= 0.0025

$t_{critical\ (20,.0025)}$= 5.60

compare intact with surgery 1 (BTS)
t= 6.17

compare intact with surgery 2 (HARMS)
t= 5.93

compare intact with surgery 3 (destabilized)
t= -10.28

compare surgery 1 (BTS) with surgery 2 (HARMS)
t= -0.23

compare surgery 1 (BTS) with surgery 3 (destabilized)
t= -16.45

compare surgery 2 (HARMS) with surgery 3 (destabilized)
t= -16.21

Beyond $F_{critical}$

Lateral Bending

	intact		Surgery 1		Surgery 2		Surgery 3
n=	6	n=	6	n=	6	n=	6
mean=	14.10	mean=	3.60	mean=	4.00	mean=	31.60
Sa^2=	8.41	Sb^2=	3.24	Sc^2=	1.96	Sc^2=	21.16
sd=	2.90	sd=	1.80	sd=	1.40	sd=	4.60

		F_{test} or	
alpha=	0.01	VR=	118.75
K=	4	$F_{(0.90,3,20)}$=	2.38
N=	24	$F_{(0.95,3,20)}$=	3.10
X=	13.33	$F_{(0.99,3,20)}$=	4.94
Sb^2=	1032.22	since VR> Fcritical, we reject the null and	
Sw^2=	8.69	accept the alternative because p<0.01	

Bonferroni - two tailed

(alpha/4)= 0.0025

$t_{critical\ (20,.0025)}$= 5.60

compare intact with surgery 1 (BTS)
t= 6.17

compare intact with surgery 2 (HARMS)
t= 5.93

compare intact with surgery 3 (destabilized)
t= -10.28

compare surgery 1 (BTS) with surgery 2 (HARMS)
t= -0.23

compare surgery 1 (BTS) with surgery 3 (destabilized)
t= -16.45

compare surgery 2 (HARMS) with surgery 3 (destabilized)
t= -16.21

Beyond $F_{critical}$